# MALT1 controls attenuated rabies virus by inducing early inflammation and T cell activation in the brain

**Running title**: MALT1 is required to control attenuated rabies virus

E. Kip,[1,2,3] J. Staal,[2,3] L. Verstrepen,[2,3] H. G. Tima,[4] S. Terryn,[1] M. Romano,[4] K. Lemeire,[2,3] V. Suin,[1] A. Hamouda,[1] M. Kalai,[1,6] R. Beyaert,[2,3]*[#] S. Van Gucht[1,5]*[#]

[1] National Reference Center of Rabies, Viral diseases, Communicable and Infectious Diseases, Scientific Institute of Public Health (WIV-ISP), Brussels, Belgium
[2] Center for Inflammation Research, Unit of Molecular Signal Transduction in Inflammation, VIB, Ghent, Belgium
[3] Department of Biomedical Molecular Biology, Ghent University, Ghent, Belgium
[4] Scientific Service Immunology, Communicable and Infectious Diseases, Scientific Institute of Public Health (WIV-ISP), Brussels, Belgium
[5] Laboratory of Virology, Department of Virology, Parasitology and Immunology, Faculty of Veterinary Medicine, Ghent University, Ghent, Belgium
[6] Current address: Clinical Laboratory Sciences (CLS), Clinical Evidence Generation (CEG) – R&D, GSK Vaccines, Rixensart, Belgium

*R.B. and S.V.G. are co-senior authors.

[#]Corresponding authors:

Rudi Beyaert, VIB-UGent Center for Inflammation Research, Technologiepark 927, B-9052 Gent, Belgium; Tel.: +32 93313770; E-mail: rudi.beyaert@irc.vib-ugent.be

Steven Van Gucht, National Reference Center of Rabies, Communicable and Infectious Diseases, Scientific Institute of Public Health (WIV-ISP), Engeland St. 642, B-1180 Brussels, Belgium; Tel.: +32 23733256, Fax: +32 23733286; E-mail: steven.vangucht@wiv-isp.be

## ABSTRACT

MALT1 is involved in the activation of immune responses as well as in the proliferation and survival of certain cancer cells. MALT1 acts as a scaffold protein for NF-κB signalling and a cysteine protease that cleaves substrates, further promoting the expression of immunoregulatory genes. Deregulated MALT1 activity has been associated with autoimmunity and cancer, implicating MALT1 as a new therapeutic target. While MALT1 deficiency has been shown to protect against experimental autoimmune encephalomyelitis, nothing is known about the impact of MALT1 on virus infection in the central nervous system. Here, we studied infection with an attenuated rabies virus (ERA) and observed increased susceptibility with ERA in MALT1$^{-/-}$ mice. Indeed, following intranasal infection with ERA, wild-type mice developed mild transient clinical signs with recovery at 35 DPI. Interestingly, MALT1$^{-/-}$ mice developed severe disease requiring euthanasia around 17 DPI. A decreased induction of inflammatory gene expression and cell infiltration and activation was observed in MALT1$^{-/-}$ mice at 10DPI as compared to MALT1$^{+/+}$ infected mice. At 17 DPI, however, inflammatory cell activation was comparable to the one observed in MALT1$^{+/+}$ mice. Moreover, MALT1$^{-/-}$ mice failed to produce virus-neutralizing antibodies. Similar results were obtained with specific inactivation of MALT1 in T cells. Finally, treatment of wild-type mice with mepazine, a MALT1 protease inhibitor, also led to mortality upon ERA virus infection. These data emphasize the importance of early inflammation and activation of T cells through MALT1 for controlling the virulence of an attenuated rabies virus in the brain.

## IMPORTANCE

Rabies virus is a neurotropic virus which can infect any mammal. Annually, 59000 people die from rabies. Effective therapy is lacking and hampered by gaps in the understanding of virus pathogenicity. MALT1 is an intracellular protein involved in innate and adaptive immunity, and an interesting therapeutic target because MALT1-deregulated activity has been associated with autoimmunity and cancers. The role of MALT1 in viral infection is however largely unknown. Here, we study the impact of MALT1 on virus infection in the brain, using the attenuated ERA rabies virus in different models of MALT1 deficient mice. We reveal the importance of MALT1-mediated inflammation and T cell activation to control ERA virus, providing new insights in the biology of MALT1 and rabies virus infection.



## KEYWORDS

Rabies virus, ERA, MALT1, neuroinflammation, immunity

## INTRODUCTION

The paracaspase MALT1 (mucosa-associated lymphoid tissue lymphoma translocation gene 1) is an intracellular protein that mediates nuclear factor κB (NF-κB) and p38/JNK MAP kinase signalling in response to multiple stimuli, including antigen receptor activation in lymphocytes, dectin-driven dendritic cell activation, and thrombin- and angiotensin-induced activation of fibroblasts and endothelial cells (1). In resting cells, MALT1 is constitutively associated with the caspase recruitment domain (CARD)-containing protein BCL10 and upon stimulation forms a complex with one of the CARD-containing proteins CARD9, CARD10 (CARMA3), CARD11 (CARMA1), or CARD14 (CARMA2), depending on the cell type and stimulus (2). The CARD-BCL10-MALT1 (CBM) complex acts as a scaffold for other proteins, including TRAF6, which then mediates the activation of NF-κB and p38/JNK (3). In addition to its scaffold function, MALT1 holds proteolytic activity that cleaves a limited number of proteins at well-defined sites (4). MALT1 substrates include among others, NF-κB family members (5), ubiquitin regulatory enzymes (6-8), and ribonuclease and mRNA-destabilizing proteins (9,10). MALT1 proteolytic activity is not essential for NF-κB or p38/JNK activation but further fine-tunes gene expression that contributes to immune cell activation, proliferation and survival. Because of its major role in lymphocyte activation and proliferation, targeting MALT1 proteolytic activity via small compound inhibitors is currently of high interest for the treatment of several autoimmune diseases and lymphoma (11-13).

Genetic mouse models have provided key insights into the biology of MALT1. MALT1$^{-/-}$ mice are viable, fertile and born at the expected Mendelian ratios (14,15). Their total number of T cells and the distribution of CD4$^{+}$ and CD8$^{+}$ T cells in the spleen, lymph nodes and thymus is comparable to those of wild-type (WT) mice, but T cell activation, proliferation and IL-2 production is decreased, leading to a lower number of activated T cells in the

95 periphery (15). MALT1 is also required for the development of regulatory T cells in the
96 thymus (16,17), as well as the development of marginal zone (MZ) and B1 B cells (14,15),
97 but is dispensable for the development of normal B2 B cells. MALT1$^{-/-}$ mice present impaired
98 IgM- and CD40-induced proliferation, and lower basal serum immunoglobulin levels, with
99 IgM and IgG3 showing the most pronounced reduction. A limited number of patients
100 carrying MALT1 mutations leading to severe immunodeficiency have been reported (18-20),
101 further illustrating the key role of MALT1 in innate and adaptive immunity. Finally, knock-in
102 mice expressing a so-called 'protease-dead' mutant of MALT1 in which the catalytic activity
103 is disrupted, but which can still function as a scaffold for NF-κB activation, mimic all
104 immune defects that are observed in full MALT1$^{-/-}$ mice, although to a lesser extent.
105 Surprisingly, these mice spontaneously develop autoimmunity because of a deregulated
106 effector T cell response (reviewed in (1)).

107 While genetic studies have indicated that MALT1 deficiency may lead to severe immune
108 defects, promising results upon pharmacological targeting of MALT1 in preclinical mouse
109 models of multiple sclerosis (12) and ABC-type diffuse large B cell lymphoma (11,13),
110 without obvious side effects, have stirred a lot of interest in the therapeutic targeting of
111 MALT1. However, a better understanding of the role of MALT1 in different tissues and
112 under different conditions is essential. Previous studies already showed that MALT1
113 deficiency protects against experimental autoimmune encephalitis (EAE) (12,16,17),
114 illustrating a role for MALT1 in the central nervous system (CNS). In the present study, we
115 focused on the impact of MALT1 deficiency on infection with a neurotropic virus. More
116 specifically, we investigated whether MALT1 deficiency affects the virulence of an
117 attenuated rabies virus.

118 Rabies virus is a highly neurotropic negative single-stranded RNA virus that belongs to
119 the *Genus Lyssavirus*, *Familia Rhabdoviridae* (21). Rabies virus normally causes a highly

120 lethal infection of the brain, which escapes control from the immune system (22). The virus
121 still kills at least 59000 humans each year and remains an important public health problem
122 (23). A small number of humans have survived clinical rabies virus infection (24,25),
123 suggesting that, at least under certain conditions, the immune system can clear rabies virus
124 from the brain. Evelyn–Rotnycki–Abelseth (ERA) virus is a highly attenuated rabies virus
125 laboratory strain that was first described in the sixties (26,27). In contrast to virulent rabies
126 virus strains, ERA virus induces a benign non-lethal infection of the nervous system that is
127 associated with an efficient immune response (28). The ERA strain has therefore been used
128 as a live vaccine for oral immunization of wildlife (29). Since the ERA virus strain causes a
129 non-lethal brain infection in mice and can mount protective immunity against rabies, it allows
130 to study the mechanisms by which the host can control rabies virus in the brain.

131 The role of T cell immunity in the control of rabies virus infection has been thoroughly
132 documented (30-32). To study the impact of MALT1 activity on rabies virus infection, we
133 compared the clinical and immunological effect of ERA virus infection in $MALT1^{+/+}$ and
134 $MALT1^{-/-}$ mice, as well as conditional $MALT1^{-/-}$ mice, lacking MALT1 in specific cell types
135 such as T cells, neuroectodermal cells or myeloid cells. We also examined the effect of
136 treatment of mice with mepazine, a phenothiazine derivative and reversible MALT1 protease
137 activity inhibitor (33). Our results demonstrate that MALT1 plays an important role in the
138 control of infection by attenuated rabies virus in the CNS of laboratory mice by inducing
139 neuroinflammation and by recruiting and activating $CD8^+$ and $CD4^+$ T cells within the brain
140 in the early phase of infection.

141

## MATERIALS AND METHODS

### *Mice*

MALT1$^{-/-}$ mice were generated and provided generously provided by the team of Prof. Dr. Tak Mak (15). Mice were backcrossed for more than 10 generations into the C57BL/6 background and were inter-crossed to generate MALT1$^{+/+}$, MALT1$^{+/-}$ and MALT1$^{-/-}$ offspring. Mice lacking MALT1 specifically in T cells were generated by crossing the CD4-Cre line (34) and mice in which the *MALT1* gene is flanked by two loxP Cre recombinase recognition sites (MALT1$^{FL/FL}$) on a C57BL/6 background. MALT1$^{FL/FL}$ mice were originally derived from the EUCOMM Malt1$^{tm1a(EUCOMM)Hmgu}$ strain. Mice lacking MALT1 specifically in cells from neuroectoderm origin (neurons, astrocytes and oligodendrocytes) were generated by crossing the Nestin-Cre line (35) and MALT1$^{FL/FL}$. Mice lacking MALT1 specifically in myeloid cells were generated by crossing the LysM-Cre line (36) and MALT1$^{FL/FL}$. All mice were bred and housed in filter top cages in temperature-controlled, air conditioned facilities with 14/10h light/dark cycles and food and water *ad libitum*, and used at the age of 6–12 weeks. All experimental procedures were approved by the Local Ethical Committee of the Scientific Institute of Public Health (WIV-ISP) and the Veterinary and Agrochemical Research Center (CODA-CERVA) (advice n° 070515-05).

### *Genotyping*

MALT1$^{-/-}$, $^{+/+}$ and $^{+/-}$ mice were genotyped using the primers P08_11 (GGG TAC ATC ATG GCC TGA ACA GTT G), P08_12 (TCC ACT CCA GCT CTT CTG CTA ACCAG) and P08_13 (GGG TGG GAT TAG ATA AAT GCC TGC TC), which resulted in PCR products of 900 bp for MALT1$^{+/+}$, 1000 bp for MALT1$^{-/-}$, or both for heterozygous MALT1$^{+/-}$ mice. The MALT1 Flox-allele was detected with the primers MALTcKO-F (GTT TCT CAG GTC TTT AGT TCA TGT C), CoMLT-3-R (TAT ACT CTA CAT CTC CAT GGT), MALTcKO-R

(TTG TTT TGC AGA TCT CTG CC), which resulted in PCR products of 280 bp for MALT1$^{+/+}$, 400 bp for MALT1$^{FL/FL}$, or 345 bp for MALT1$^{-/-}$ mice. The Cre allele was detected with the primers Cre-F (TGC CAC GAC CAA GTG ACA GCA ATG) and Cre-R (AGA GAC GGA AAT CCA TCG CTC G), producing a 374 bp PCR fragment. Transgenic mice were identified by PCR analysis of genomic DNA extracted from tails and amplification of the selected fragments was performed using the GoTaq G2 DNA polymerase (Promega, Madison, USA) master mix, with a typical PCR program: 5 minutes 95 °C denaturation, 35-40 cycles [30s 95 °C | 30s 55-60 °C | 60s 72 °C] and 10 minutes 72 °C for final elongation. Fragments were visualised on a 2% agarose gel.

*Virus*

The attenuated Evelyn-Rotnycki-Abelseth (ERA) virus, used as an oral vaccine for immunisation of wild life, was obtained from the American Type Culture Collection (ATCC) (Reference: VR322) (37). Viral stocks were produced in baby hamster kidney (BHK)-21 cells (Deutsche Sammlung von Mikroorganismen und Zellkulturen GmbH, Braunschweig, Germany). The lysates of infected cell cultures were centrifuged at 20,000g for 20 min at 4°C and supernatants were stored at -80°C.

*Virus titration*

Infectious rabies virus particles were titrated by endpoint dilution assay in BHK-21 cells. The measure of infectious virus titer was expressed as 50% tissue culture infective dose (TCID50)/ml and represents the the amount of virus per ml that gives rise to infection in 50% of inoculated tissue culture cells. Virus titration was performed according to the Manual of Diagnostic Tests and Vaccines for Terrestrial Animals (Office International des Epizooties, 2008).

*Virus inoculation, clinical follow up, euthanasia and sampling*

190 Mice were inoculated intranasally with ERA virus using $10^5$ $TCID_{50}$ in 25µl of PBS,
191 during brief anaesthesia with isoflurane, as described by Rosseels *et al* (38). Intranasal
192 inoculation of virus was chosen, as administration by this route results in a quick invasion of
193 the CNS. Mice were monitored once a day for signs of disease throughout the experiment
194 until 35 days post inoculation (DPI). A cumulative daily clinical score per mouse was
195 obtained by adding the scores for each parameter and ranged from 0 (no disease) to 9 (severe
196 brain disease). Disease signs were scored as follows: no signs = 0, rough hair coat = 1,
197 depression / isolation from the group = 1, hunched back = 1, slow movement = 1, paresis in
198 the front paws = 1, uncoordinated movements = 1, no spontaneous movements = 1, paralysis
199 of hind legs = 1, no response to external stimuli (end stage) = 1. Disease progression is
200 represented by a curve of the mean cumulative score per group. Once mice reached a
201 minimum score of 6, or at pre-determined time points post virus inoculation (10DPI:
202 incubation phase and 17DPI: end stage of disease), mice were euthanized with an overdose of
203 ketamine (Ceva, Brussels, Belgium, 100 mg/kg) and xylazine (Rompun 2%, Bayer
204 Healthcare, Kiel, Germany, 9.9 mg/kg) (300µl/mouse, intraperitoneally (ip)). Upon terminal
205 anaesthesia, the blood was flushed from the circulatory system by transcardial perfusion with
206 a PBS solution. Brains were collected and divided in two halves according to a longitudinal
207 section. One half was stored at -80°C for further analysis by real time quantitative reverse
208 transcriptase polymerase chain reaction (RT-qPCR) or fluorescent antigen test (FAT), the
209 other half was submerged in 4% formaldehyde for fixation and further immunohistochemical
210 analysis. Serum was collected from mice at different time points post infection and upon
211 euthanasia for titration of virus-neutralizing antibodies. Mice that did not develop disease
212 signs were terminally anesthetised, perfused and euthanized at 35 DPI.

213 *RNA extraction and real time quantitative reverse transcriptase polymerase chain reaction*
214 *(RT-qPCR) assay for quantification of viral RNA and inflammatory gene expression.*

Seven mice per group were euthanized at each indicated time point. RNA extraction was performed using the RNeasy Mini kit (Qiagen, Hilden, Germany) according to the manufacturer's instructions. RNA concentration was calculated using Nano Vue spectrophotometry (GE Healthcare, Bucks, UK) and 100 ng was used for reverse transcription. Reverse transcription and q-PCR were performed as described by Rosseels *et al.* (38). Two primers (forward and reverse), located in the nucleoprotein N genome region were used for quantification of viral RNA. All primer sequences are listed in Table 1. All samples were analysed in duplicates. Amplification was performed on an iCycler iQ (Biorad) in a 96-well optical plate format, using the following program: 2 min at 95°C followed by 45 cycles of: 20 sec at 95°C and 30 sec at 62°C. A melting curve analysis was performed in order to verify the specificity of amplicons. Expressions of inflammatory genes were normalized using the cellular 18S rRNA housekeeping gene. Quantification of immune gene expression was performed using the comparative ΔΔCt method. The fold was calculated as $2^{-\Delta\Delta Ct}$ with $\Delta\Delta Ct = \Delta Ct_{sample} - \Delta Ct_{ctrl}$. $\Delta Ct_{sample} = Ct_{gene} - Ct_{18S}$ and $\Delta Ct_{ctrl} = Ct_{ctrl} - Ct_{18S}$ with $Ct_{ctrl}$ corresponding to the Ct of gene expression in non-infected brain. For the detection of the viral N protein's gene, delta cycle thresholds (ΔCt) values were calculated using the following formula: $\Delta Ct = Ct_{ref} - Ct_{sample}$, with $Ct_{ref}$ equal to 45, which is the maximum number of cycles of this qPCR program. A ΔCt value of 0 means no detection of viral RNA.

*Titration of neutralizing antibody by rapid fluorescent focus inhibition test (RFFIT)*

Mouse blood samples were used for measurement of neutralizing antibodies using the RFFIT according to the Manual of Diagnostic Tests and Vaccines for Terrestrial Animals (Office International des Epizooties, 2008). Neutralizing antibody titers are expressed as International Units (IU)/ml in reference to "The Second International standard for Anti-rabies Immunoglobulin", purchased from the United Kingdom National Institute for Biological

239 Standards and Control. Serum titer levels of 0.5 IU/ml or higher is an indication of
240 seroconversion.

241 *Detection of nucleocapsid antigen of rabies virus by fluorescent antigen test (FAT)*

242 The fluorescent antigen test (FAT) was performed according to the Manual of Diagnostic
243 Tests and Vaccines for Terrestrial Animals (Office International des Epizooties, 2008). Brain
244 smears were fixed with 75% acetone for 30 min at -20°C and incubated with FITC-coupled
245 anti-nucleocapsid rabbit antibody for 30 min at 37°C.

246 *Immunohistological analysis of mouse brains for expression of Iba-1, GFAP, B220, CD3 and*
247 *Mac-3*

248 Virus-inoculated mice and PBS-inoculated mice were transcardially perfused with PBS.
249 Brains were removed, immersed in 4% paraformaldehyde, dehydrated, and embedded in
250 paraffin blocks. Sections of 2µm were realized and microglial cells, astrocytes, B cells, T
251 cells and macrophages were detected using specific antibodies: rabbit anti-Iba-1 (WAKO
252 Chemicals, Fuggerstraβe, Germany), rabbit anti-GFAP (DAKO - Agilent Technologies,
253 Santa Clara, CA, USA), rat anti-B220 (eBioscience - Thermo Fisher Scientific,
254 Waltham, MA USA), rabbit anti-CD3 (DAKO - Agilent Technologies, Santa Clara, CA,
255 USA) and rat anti-Mac-3 (BD Pharmingen, San Diego, CA, USA), respectively. Sections
256 were rehydrated and incubated in 10mM citrate buffer for 10 min at 95°C. To remove
257 endogenous peroxydase, tissue sections were treated with 3% $H_2O_2$ in methanol. To block
258 non-specific reactions, each section was treated with 5% goat serum in antibody diluent
259 (DAKO - Agilent Technologies, Santa Clara, CA, USA) for 30 min. Primary antibody was
260 diluted in 5% goat serum in antibody diluent with the dilution depending on the staining
261 realized (Iba-1: 1/1000, CD3: 1/200, MAC-3: 1/250, B220: 1/1000, GFAP: 1/200 000) and
262 incubated on brain sections overnight at 4°C. Goat anti-rabbit (DAKO - Agilent

Technologies, Santa Clara, CA, USA) or goat anti-rat (BD Pharmingen, San Diego, CA, USA) secondary antibodies conjugated to biotin were diluted at 1:500 in block buffer and added for 45 min-1h to the sections. Drops of avidin/biotin-based peroxidase system Vectastrain® Elite® ABC (Vector laboratories, Burlingame, CA, USA) were added to each section for 30 min. Finally antibody was visualized using 3-3'-diaminobenzidine (DAB, DAKO - Agilent Technologies, Santa Clara, CA, USA) until specific staining appeared; slides were counterstained with hematoxylin, dehydrated and mounted with a xylene-based mounting medium. Sections without primary antibody were taken along as controls.

*Immunophenotyping of leukocytes*

Immune cells were extracted from the brain at 10 DPI as described (39). In brief, brains were collected and single-cell suspensions were prepared by gently pressing the organs in HBSS through a nylon mesh (mesh size 100µm). After centrifugation, cells were placed in collagenase-DNase for 1h. After washing, the suspension was centrifuged in 25% Percoll (Sigma Aldrich, St Louis, MO, USA), the myelin layer was removed and cells were suspended in HBSS containing 10% FCS. Red blood cell lysis buffer was added to the cell pellet to eliminate erythrocytes. Cells were washed twice with FACS buffer (PBS containing 10% FCS and 0.1% $NaN_3$) and incubated with FcγII/III receptor blocking anti-CD16/CD32 (clone 2.4G2, BD Biosciences, San Jose, CA, USA) for 15 minutes at 4°C. Cells were then incubated for 30 minutes at 4°C protected from light with viability dye (Thermofisher) and the appropriate dilutions of the following antibodies Alexa fluor 488-anti CD11b (clone M1/70), Brilliant Violet-421 anti-CD45 (clone 104), PE-anti-CD49b (clone DX5), APC-Cy7-anti-CD3 (clone 145-2C11), PerCP-Cy5.5-anti-CD8 (clone 53-6.7), APC-anti-CD4 (clone GK1.5), PE-Cy7-anti-CD86 (clone GL1). The stained cells were washed twice in FACS buffer, fixed with 4% paraformaldehyde and analyzed in a BD FACSVERSE Flow

cytometer. Data were analyzed using BD FACSuite software. Antibodies were from BD Pharmingen or Thermofisher.

*Activation of T cells*

For analysis of T cell activation in the brain, collected leukocytes were cultured in the presence of 1µg/ml anti-CD28 (clone 37.51), 1µg/ml of anti-CD49d (clone 9C10 (MFR4.B)), 10 µg/ml of ERA inactivated antigens and Brefeldin A (Thermofisher) for 5h at 37°C. Cells were then harvested, washed twice and suspended in FACS buffer containing FcγII/III receptor blocking anti-CD16/CD32 (clone 2.4G2, BD Biosciences, San Jose, CA, USA) for 15 min at 4°C. Cells were stained with viability dye and a cocktail of extracellular antibodies (Brilliant Violet-421 anti-CD45 (clone 104), APC-Cy7-anti-CD3 (clone 145-2C11), APC-anti-CD4 (clone GK1.5), PerCP-Cy5.5-anti-CD8 (clone 53-6.7)). Cells were then washed twice with FACS buffer and permeabilized using Cytofix/Cytoperm kit (BD pharmingen). Cells were subsequently suspended in 1X Perm Wash buffer (BD pharmingen) containing a cocktail of PE-anti-IFNγ (clone XMG1.2), Alexa Fluor 488-anti-IL-17A (clone TC11-18H10) and PE-Cy7-GranzymeB (NGZB)). Isotype control and Fluorescence Minus One controls (FMO) staining were done in parallel. Cells were then washed twice and fixed with 4% paraformaldehyde. Samples were examined using BD FACSVERSE Flow cytometer and analyzed with BD FACSuite software. Antibodies were from BD Pharmingen or Thermofisher.

*Serum transfer by intraperitoneal injection*

Serum was collected at 35 DPI from immune C57BL/6 mice infected with $10^5$ $TCID_{50}$/25µl ERA virus. $MALT1^{-/-}$ mice received 500µl of serum i.p. on day 10 after virus challenge. Serum of naïve mice was used as a control. Mouse sera were heat-inactivated prior to administration (30 min at 56°C).

311 *Treatment with mepazine*

312 Mice were randomly treated with either mepazine or 0.9% NaCl. Mepazine (Chembridge)
313 was solubilized in NaCl 0.9% at a concentration of 2 mg/ml. Mice were injected i.p. daily
314 with 200 µl (16 mg/kg) starting 2 days before ERA virus inoculation until the end of the
315 experiment. Mice were monitored once a day for signs of disease throughout the experiment.

316 *Statistical analyses*

317 Statistical analysis was performed using the Student's t test for unpaired data or the 2-way
318 ANOVA followed by a Sidak multiple comparison test in GraphPad Prism7. Logrank test
319 was used to analyse Kaplan-Meier survival curves.

320





Journal of Virology JVI Journal of Virology

## RESULTS

### *Attenuated ERA virus becomes virulent in MALT1$^{-/-}$ mice*

Intranasal inoculation of ERA virus in wild-type C57BL/6 mice resulted in a clinically benign infection with, as expected, complete survival (40) (Figure 1A-B). Minor clinical signs were observed at day 10 (rough hair coat and a slightly reduced reactivity) and the general appearance (rough hair coat) improved rapidly (11DPI). Nevertheless most mice remained slightly less reactive throughout the follow-up period (35DPI) resulting in a clinical score of 1. Differently, ERA virus inoculated MALT1$^{-/-}$ mice presented the first clinical signs around 15 DPI and developed severe disease, characterized by limb paralysis and depression, requiring euthanasia at 17 or 18 DPI. These data indicate that MALT1 is necessary to control infection with ERA. Viral loads were analysed in total brain, by RT-qPCR and FAT, and in olfactory bulbs, cerebrum and cerebellum by RT-qPCR (Figure 2A-D). At 10 DPI, viral loads were similar in the brains of MALT1$^{-/-}$ and MALT1$^{+/+}$ mice (Figure 2C). At 17 DPI, which corresponds with the end stage of disease in MALT1$^{-/-}$ mice, a significantly higher viral load was observed in the different parts of MALT1$^{-/-}$ mouse compared to MALT1$^{+/+}$ brains (Figure 2D). Fluorescence staining of the viral N protein yielded a similar signal in MALT1$^{-/-}$ and MALT1$^{+/+}$ brains at 10DPI, whereas at 17DPI more fluorescent foci were observed in MALT1$^{-/-}$ brains (Figure 2E), in agreement with the results obtained by RT-qPCR. These results show that deficiency of MALT1 leads to a progressive and lethal increase of ERA viral load in the brain, resulting in severe clinical signs.

### *Anti-viral and inflammatory gene expression is severely disrupted in the brain of MALT1$^{-/-}$ mice at the pre-symptomatic phase of infection*

To further analyze the increased virulence of ERA virus in MALT1 deficient mice, virus-induced expression of several immune response genes in the brain was assessed. The mRNA

levels of interferons (IFNβ, IFNγ), pro-inflammatory cytokines (TNF, IL-1β, IL-12, IL-23), chemokines (MIP2, MCP1, CXCL10), Th1 associated genes (IFNγ, t-bet), T-reg associated genes (Foxp3), inflammasome components (NLRP3, caspase-1), T cell markers (CD4 and CD8), and iNOS enzyme were measured in the brains of MALT1$^{+/+}$ or MALT1$^{-/-}$ mice at different time-points after infection and compared with mRNA levels in the corresponding uninfected controls. As shown in figure 3, no upregulation of IL-12 could be observed. At 10 DPI, expression of all other investigated genes was higher following ERA virus infection in infected compared to non-infected mice. In contrast, at comparable time points, virus-induced expression of the same genes was much less pronounced in the brains of MALT1$^{-/-}$ mice, with the exception of MCP1, MIP2, CD4, and IL-23 that were expressed to a similar extent. Absence of Foxp3 expression reflects the known lack of thymic regulatory T cells in MALT1$^{-/-}$ mice (41), while absence of CD8 and IFNγ indicates a defective cytotoxic T cell response. The anti-viral IFN-β response and pro-inflammatory gene expression were also almost completely absent. At 17 DPI, virus-induced gene expression was in most cases less pronounced compared to 10 DPI and differences between MALT1$^{+/+}$ and MALT1$^{-/-}$ were more gene-dependent: expression of IFN-β and Foxp3 was absent, whereas expression of TNF and CXCL10 was significantly higher in the brains of MALT1$^{-/-}$ mice compared to MALT1$^{+/+}$ mice. The latter results are in line with the high viral loads detected at 17DPI in the brain of MALT1$^{-/-}$ as compared to MALT1$^{+/+}$ mice (Figure 2). Together, these results suggest that at the early stage of infection (10 DPI) anti-viral and inflammatory immune responses are severely disrupted in MALT1$^{-/-}$ mice.

*MALT1 deficiency is associated with decreased infiltration and activation of inflammatory and immune cells in the brain at the pre-symptomatic phase of infection*

368 To investigate if the above described defects in virus-induced cytokine and chemokine
369 expression in MALT1$^{-/-}$ mice were also associated with an altered recruitment and activation
370 of inflammatory cells, immunohistological analysis for different inflammatory cell markers
371 was performed on brain sections obtained at 10 DPI and 17 DPI from ERA-infected
372 MALT1$^{+/+}$ and MALT1$^{-/-}$ mice in comparison to PBS-inoculated control mice (Figure 4).
373 Microglia cells, which are the resident macrophages of the CNS, and astrocytes, which are
374 the most abundant glial cell population, typically both respond to injury and infection by
375 acquiring an activated phenotype, defined by morphologic changes, migration and
376 proliferation (42,43). Staining for the microglia cell marker Iba1 revealed an increased
377 number of activated microglia at 10 and 17 DPI in MALT1$^{+/+}$ mice compared to non-infected
378 brains. Microglia activation is demonstrated by the typically bigger cell body and shorter and
379 thicker branch processes. Resting microglial cells, observed mainly in non-infected mice,
380 were characterized by their smaller cell bodies and long and ramified branch processes. In
381 ERA-infected MALT1$^{-/-}$ mice, the number of activated microglia cells was less pronounced at
382 both 10 and 17 DPI compared to MALT1$^{+/+}$ mouse brains. Astrocyte activation was also
383 evident in ERA-infected MALT1$^{+/+}$ mice as demonstrated by enhanced GFAP
384 immunoreactivity. At 10 DPI, GFAP staining was observed in the white matter of the
385 cerebellum, whereas at 17 DPI, GFAP staining was observed in the white matter and in the
386 outer layer of the grey matter. In ERA-infected MALT1$^{-/-}$ mice, astrocyte activation in the
387 outer layer of the grey matter was slightly reduced at 17 DPI.

388 Infiltration of CD3$^{+}$ T cells and Mac-3$^{+}$ macrophages was observed at 10 DPI in ERA-
389 infected MALT1$^{+/+}$ mice. The T cell infiltrates persisted at 17 DPI, whereas macrophage
390 infiltrates were no longer visible. T cell and macrophage infiltration was much less
391 pronounced in ERA-infected MALT1$^{-/-}$ mice at 10 DPI, but similar levels of T cells were
392 detected in ERA-infected MALT1$^{+/+}$ and MALT1$^{-/-}$ mice at 17 DPI. B220$^{+}$ B cells were

393 detectable around the blood vessels and in the choroid plexus, but not in the brain
394 parenchyma, at 10 DPI and 17 DPI in ERA-infected MALT1$^{+/+}$. In contrast, almost no B cells
395 were detected in ERA-infected MALT1$^{-/-}$ mice, neither around blood vessels nor in the
396 choroid plexus. As expected, CD3$^{+}$, B220$^{+}$ or Mac-3$^{+}$ staining was not detected in PBS-
397 inoculated control mice. For all stainings, results were similar in cerebellum and
398 hippocampus.

399 Inflammatory cell infiltration was also assessed by flow cytometric analysis of brain
400 leukocytes at 10 DPI. As shown in figure 5A, strong leukocyte infiltration was observed in
401 ERA-infected MALT1$^{+/+}$ mice as compared to non-infected mice. A comparatively lower
402 number of leukocytes was detected in infected MALT1$^{-/-}$ mice. Analysis of cell populations
403 revealed strong infiltration of microglial cells (CD45$^{int}$CD11b$^{+}$),
404 monocytes/macrophages/DCs (CD45$^{high}$CD11b$^{+}$), NK cells (CD49$^{+}$CD3$^{-}$), NKT cells
405 (CD49b$^{+}$CD3$^{+}$), and T cells (CD49b$^{-}$CD3$^{+}$) with a high proportion of CD8$^{+}$ T cells and a few
406 CD4$^{+}$ T cells (Figure 5B and C) in ERA-infected MALT1$^{+/+}$ mice. Analysis of costimulatory
407 markers such as CD86 showed that microglia and monocytes/macrophages/DCs were highly
408 activated, which was confirmed by analysing the mean fluorescence intensity (M.F.I.) of the
409 CD86 marker (Figure 5C). In ERA-infected MALT1$^{-/-}$ brains, the absolute number of total
410 leukocytes was much lower compared to ERA-infected MALT1$^{+/+}$ brains (Figure 5A), which
411 is also reflected by lower numbers of CD8$^{+}$ T cells, NK cells, NKT cells, activated
412 monocytes/macrophages/DCs and activated microglia. No significant difference was
413 observed for CD3$^{+}$CD4$^{+}$ T cells (Figure 5B and C), which is in line with equal CD4 mRNA
414 expression in MALT1$^{+/+}$ and MALT1$^{-/-}$ mouse brains (Figure 3). Furthermore, *in vitro*
415 stimulation of leukocytes isolated from ERA-infected MALT1$^{+/+}$ brains with inactivated ERA
416 virus showed that T cells express IL-17, IFN-γ and granzyme B, suggesting the recruitment
417 of Th1, Th17 and CD8$^{+}$ T cells. In contrast, leukocytes from ERA-infected MALT1$^{-/-}$ mice

418 produced significantly less IL-17, granzyme B and IFN-γ (Figure 6). Altogether, these data
419 illustrate that MALT1 deficiency is associated with decreased infiltration and activation of
420 inflammatory and immune cells in the brain upon ERA virus infection.

421 *MALT1 deficiency is associated with a defective anti-viral humoral immune response*

422 To investigate if MALT1 deficiency also affects the humoral immune response against
423 ERA virus we measured rabies virus neutralising antibodies (VNA) in the serum. VNA were
424 detected in the blood of MALT1$^{+/+}$ infected mice at 17 DPI (1.90 +- 1.30 IU/ml). This time
425 point was chosen because it is the end point of disease for MALT1$^{-/-}$ mice. Titers increased
426 further at 35 DPI (6.53 +- 3.12 IU/ml) (Figure 7). However, most MALT1$^{-/-}$ mice failed to
427 produce VNA (<0.5 IU/ml). Low levels of VNA (0.85 IU/ml) could be detected in two
428 MALT1$^{-/-}$ mice at 17 DPI, but this made no difference on infection and disease outcome.
429 To further assess the role of antibodies in the protection against ERA virus in the brain, we
430 tested whether transfer of serum from immunized MALT1$^{+/+}$ mice could infer protection in
431 MALT1$^{-/-}$ mice. Pooled immune serum (4.8 IU/ml, 0.5 ml/mouse ip) was transferred to ERA-
432 infected MALT1$^{-/-}$ mice at 10 DPI, which corresponds to the time point when MALT1$^{+/+}$ mice
433 normally start to produce VNA after infection with ERA virus (Figure 8A). Transfer of
434 immune serum was unable to rescue the MALT1$^{-/-}$ mice from lethal infection (Figure 8B).
435 These results suggest that antibodies alone are not sufficient to confer protection and that
436 cell-mediated immunity is also necessary.

437 *MALT1 deficiency in T cells is sufficient to render ERA virus neurovirulent*

438 MALT1$^{-/-}$ mice were previously shown to have a normal number of T cells but their
439 capacity to be activated is impaired (15). We therefore hypothesized that MALT1 in T cells
440 might be important to control ERA virus. This was investigated by using T cell specific
441 MALT1$^{-/-}$ mice that were generated by crossing CD4-Cre mice with mice in which the

442 MALT1 gene is flanked by two loxP Cre recombinase recognition sites (MALT1$^{FL/FL}$)
443 (Figure 9A). In contrast to wild-type littermates (CD4-Cre$^{+/+}$ MALT1$^{FL/FL}$), infection of T cell
444 specific MALT1$^{-/-}$ mice (CD4-Cre$^{tg/+}$ MALT1$^{FL/FL}$) with ERA virus led to severe disease and
445 death between 15 DPI and 17 DPI (Figure 9B), similarly to the phenotype observed in
446 MALT1 full knock-out mice (Figure 1). In addition, we observed that most of the T cell
447 specific MALT1$^{-/-}$ mice did not mount an antibody response (Figure 9C). Indeed, only one
448 mouse developed a low level of VNA (0.99 IU/ml). Accordingly, we also observed a
449 significant increase of viral load in CD4-Cre$^{tg/+}$ MALT1$^{FL/FL}$ compared to their wild-type
450 littermates (CD4-Cre$^{+/+}$ MALT1$^{FL/FL}$) (Figure 9D). These results confirm the importance of
451 the activation of CD4$^{+}$ and CD8$^{+}$ T cells through MALT1 to control ERA virus in the CNS.
452 Theoretically, impaired signalling in neurons or myeloid cells could also be responsible for
453 the increased pathogenicity of ERA virus in MALT1$^{-/-}$ mice. Mice specifically lacking
454 MALT1 in myeloid cells (LysMCre$^{tg/+}$ MALT1$^{FL/FL}$) or cells of neuro-ectodermal origin
455 (neurons, astrocytes or oligodendrocytes; Nestin-Cre$^{tg/+}$ MALT1$^{FL/FL}$) were therefore also
456 generated and analyzed in similar infection experiments (Figure 9A). Infection of Nestin-
457 Cre$^{tg/+}$ MALT1$^{FL/FL}$ and LysMCre$^{tg/+}$ MALT1$^{FL/FL}$ mice gave survival results comparable to
458 those of wild-type littermates, excluding a role for MALT1 in neurons, astrocytes,
459 oligodendrocytes or myeloid cells (Figure 9B). Together, our data demonstrate the
460 importance of MALT1-mediated T cell activation to control infection with a live attenuated
461 rabies virus in the brain.

462 *Pharmacological inhibition of MALT1 increases virulence of ERA virus*

463 MALT1$^{-/-}$ mice lack both MALT1 scaffold and MALT1 catalytic activities. To better
464 delineate the specific role of MALT1 proteolytic activity in the control of ERA virus, we also
465 tested the effect of inhibition of MALT1 catalytic activity using the small compound inhibitor
466 mepazine. Wild-type mice were treated daily with mepazine starting two days before virus

inoculation and lasting until the late stage of disease (Figure 10A). Control mice were treated with 0.9% NaCl. Part of the mepazine-treated mice (4/7) developed severe disease and had to be euthanized between 12 and 15 DPI, while the remaining mice developed only mild disease and survived the infection (Figure 10B). At sacrifice, CNS viral loads of the mepazine-treated mice with severe disease were significantly higher than in untreated mice and reached similar levels as observed previously in MALT1$^{-/-}$ mice (Figure 10C and 2B). At 35 DPI, surviving mepazine-treated mice and control mice presented similarly low viral loads (Figures 10C). High levels of virus neutralizing antibodies were detected in the blood of the surviving mepazine-treated mice (>10 IU/ml) and control mice (8.86 +- 2.28 IU/ml), but not in the mepazine-treated mice that developed severe disease and died (0.45 +- 0.30 IU/ml) (Figure 10D). These data demonstrate that MALT1 proteolytic activity is essential for a proper immune response and the control of rabies virus infection in the CNS.

## DISCUSSION

Although attenuated vaccines are often used to immunize man and animal, there always remains a risk that they become pathogenic again either by acquisition of mutations or because of increased susceptibility of the host, as has been reported for attenuated rabies vaccines in wildlife (37,44-47). A better understanding of the immunological mechanisms that control attenuated rabies virus in the CNS is therefore of immediate interest. Our data demonstrate an important protective role for paracaspase MALT1-mediated signalling in the response to infection with the attenuated rabies virus ERA by mediating neuroinflammation at the early phase of infection. More specifically, we show that MALT1 deficiency in mice decreases cerebral immune responses at the early phase of infection as evidenced by reduced microglial, astroglial and T cell activation, less infiltration of macrophages and $CD8^+$ T cells, and diminished expression of NF-κB regulated pro-inflammatory mediators in the brain at 10 DPI. At a later phase of infection (17 DPI), however, immune cell infiltration and activation were comparable between $MALT1^{+/+}$ and $MALT1^{-/-}$ mice, indicating that immune cells can still be activated and infiltrate the brain in $MALT1^{-/-}$ infected mice, but with delayed kinetics as compared to $MALT1^{+/+}$ mice. In agreement with the curtailed immune response, $MALT1^{-/-}$ mice developed severe disease, characterized by severe depression and paralysis and requiring human euthanasia, whereas $MALT1^{+/+}$ mice developed only mild disease resolving at 11 DPI, characterized by transiently reduced activity. Similar results were observed in conditional knock-out mice lacking MALT1 specifically in T cells. In contrast, mice lacking MALT1 specifically in neuroectodermal cells or myeloid cells survived the infection. Finally, also pharmacological inhibition of MALT1 increased the pathogenicity of ERA virus. Together, our results demonstrate a key role for MALT1-dependent T cell activation in the control of attenuated rabies virus.

503 It is important to mention that T cell-specific MALT1$^{-/-}$ mice lack MALT1 in both CD4$^{+}$
504 and CD8$^{+}$ T cells, since CD4-Cre is expressed during the double positive phase of T cell
505 development. CD8+ T cells were the most recruited T cell population in the brain during
506 ERA virus infection in wild-type mice. It has been shown before that CD8$^{+}$T cells are
507 required for the early production of cytokines at the site of infection, contribute to the
508 clearance of rabies virus from the CNS by enhancing IFN-γ production and the CNS
509 inflammatory response, and kill infected cells by the release of granzyme B (48).
510 Consequently, viral loads were found to be higher in CD8$^{+}$ T cell deficient mice (48). In
511 MALT1$^{-/-}$ mice, significantly less CD8$^{+}$ T cells were recruited, whereas the number of CD4$^{+}$
512 T cells remained the same as in MALT1$^{+/+}$ mice. In contrast with others who have shown that
513 rabies virus infection in CD8$^{+}$ T cell deficient mice remains sub-lethal (48), we observed
514 lethal disease in MALT1$^{-/-}$ mice, suggesting that decreased activation of CD4$^{+}$ T cell subsets
515 also contributes to the observed sensitization in MALT1$^{-/-}$ mice. In this context, ERA rabies
516 virus infection increased expression of the transcription factor t-bet and IFN-γ in the CNS,
517 which is indicative for infiltration of CD4$^{+}$ Th1 cells. Th1 cells were previously shown to be
518 essential for the rapid clearance of attenuated rabies virus from the CNS (49), and the blunted
519 expression of t-bet and IFN-γ in MALT1$^{-/-}$ mice may thus be associated with the increased
520 lethality. We also found evidence for increased Th17 infiltration and IL-17 production in the
521 CNS of ERA rabies virus infected mice. IL-17 in the brain of mice infected with a laboratory-
522 attenuated rabies virus has previously been reported to enhance blood-brain barrier
523 permeability and viral clearance (50-52). Interestingly, IL-17 levels in the brains of ERA-
524 infected MALT1$^{-/-}$ mice were lower compared to MALT1$^{+/+}$ mice, suggesting that MALT1
525 deficiency may decrease blood-brain barrier permeability, which on its turn may contribute to
526 the reduced infiltration of inflammatory cells in the brain of infected MALT1$^{-/-}$ mice. Loss of
527 MALT1 has formerly been shown to also interfere with T cell infiltration and expression of

528 IL-17 in experimental autoimmune encephalitis (EAE) in mice, a well-known model of
529 multiple sclerosis (16,17). In this case, MALT1 inhibition was shown to protect against EAE
530 by blunting T-cell mediated autoimmunity.

531 Effective clearance of rabies virus requires the rapid production of neutralizing antibodies
532 (48). ERA-infected MALT1$^{-/-}$ mice failed to mount neutralizing antibodies. The same was
533 true for conditional knock-out mice lacking MALT1 specifically in T cells, illustrating that
534 production of neutralizing antibodies against ERA virus is T cell dependent. Although rabies
535 virus neutralizing antibodies are important for virus clearance, passive immunisation of
536 MALT1$^{-/-}$ mice failed to rescue the mice. *In situ* production of antibodies by B cells in the
537 brain (53) or active permeabilisation of the blood-brain barrier is most likely required for
538 antibodies to be effective against rabies virus (54). On the other hand, cellular immunity as
539 described above is probably also required to control the virus in the brain. Together, these
540 findings implicate that in the future, besides neutralizing antibodies, markers for cellular
541 immunity should also be considered to assess vaccine efficacy and anti-rabies immunity.

542 A hypothetical model for the impact of MALT1 inactivation on ERA rabies virus-induced
543 immune responses in the brain is depicted in figure 11. The high level of cytokines and
544 inflammation in wild-type mice at 10 DPI with ERA virus, which coincides with some mild
545 disease signs, together with the infiltration of activated T cells in the brain might be key for
546 effective control of the infection. MALT1$^{-/-}$ mice presented less infiltration of activated T
547 cells and inflammatory cytokine production in the brain and a significant reduction of CD8$^{+}$ T
548 cell, NK cell and NKT cell infiltration. We propose that the reduction of immune cell
549 infiltration in the brain, together with the lack of a peripheral humoral immune response, are
550 at the origin of the higher viral loads and severe disease in MALT1$^{-/-}$ mice.

551 The fact that MALT1 deficiency reduces neuroinflammation in the brain might also be of
552 interest in the context of therapeutic modulation of other neurological pathologies involving

553 neuroinflammation such as Alzheimer's disease (55), Parkinson's disease (56), multiple
554 sclerosis (57), stroke (58) and neuropsychiatric diseases like depression, schizophrenia and
555 autism (59,60). In this context, the allosteric MALT1 inhibitor mepazine has already been
556 shown to have a therapeutic effect in EAE (12). At the same time, however, our results
557 indicate that MALT1 inhibitors can also increase the risk for severe virus infection in the
558 brain or severe adverse effects upon vaccination with attenuated rabies viruses. Indeed,
559 mepazine treatment of ERA-infected mice led to susceptibility to virulence of ERA virus in
560 more than half of the mice. It should be mentioned that, similar to Nagel *et al* (11), in our
561 study mice were treated with 16 mg mepazine/kg body weight every 24 hours. Considering
562 the relatively short half-life of mepazine, a more frequent treatment schedule may still lead to
563 stronger sensitizing effects for ERA infection. Next to pharmacological MALT1 inhibition,
564 also mutations in MALT1 leading to MALT1 deficiency may sensitize an attenuated rabies
565 virus to neurovirulence. To date, a limited number of MALT1 deficient patients have been
566 described (18-20), each presenting with severe combined immunodeficiency and being highly
567 susceptible to fungal, bacterial and viral infections. Moreover, other mutations may be less
568 disruptive and only become apparent under certain conditions. It should be mentioned,
569 however, that rabies vaccination in humans uses only inactivated vaccines. Therefore, the use
570 of MALT1 inhibitors or MALT1 deficiency in combination with rabies vaccination in
571 humans would not impose any risks. As it remains to be seen if our findings with an
572 attenuated rabies virus also apply to other attenuated viruses, it is currently premature to
573 generalize our findings to other attenuated virus vaccines. In future studies it will be
574 interesting to also analyse the effect of MALT1 deficiency on infection with virulent rabies
575 virus or other viruses.

## ACKNOWLEDGMENTS

This work was supported by the Belgian Science Policy Office (BELSPO) under the program "Interuniversity Attraction Poles" (IAP) Phase VII (DISCOBEL IAP-7/32 project) and the European Union's Horizon 2020 research and innovation programme under RABYD-VAX grant agreement No 733176. The National Reference Centre of Rabies is partially supported by the Belgian Ministry of Social Affairs through a fund from the Health Insurance System. Work in the lab of R.B. is supported by grants from the VIB, the Fund for Scientific Research Flanders (FWO), and the Ghent University Concerted Research Actions (GOA).

A. Francart is gratefully acknowledged for her support with the mice experiments. S. Roels and M. Paluka are greatly acknowledged for their help with brain sections.

E.K., S.V.G. and R.B. conceived the study, designed experiments and wrote the manuscript. E.K. performed experiments, analyzed data and designed the figures. J.S. generated the mouse models used in this study and J.S. and L.V. edited the manuscript. E.K. bred the mice and E.K. and A.H. realized the genotyping and RT-qPCR experiments. K.L. performed the immunohistochemistry and E.K. performed the analysis. E.K. and H.G.T. performed the flow cytometry experiments and analysis. M.R. and S.T. edited the manuscript. V.S., J.S., L.V., M.R., S.T., S.V.G., R.B. and M.K. helped in the experimental design with scientific discussions.

## REFERENCES


1. **Demeyer, A., J. Staal, and R. Beyaert**. 2016. Targeting MALT1 Proteolytic Activity in Immunity, Inflammation and Disease: Good or Bad? Trends Mol.Med. **22**:135-150. doi:S1471-4914(15)00234-8 [pii];10.1016/j.molmed.2015.12.004 [doi].

2. **Blonska, M. and X. Lin**. 2011. NF-kappaB signaling pathways regulated by CARMA family of scaffold proteins. Cell Res. **21**:55-70. doi:cr2010182 [pii];10.1038/cr.2010.182 [doi].

3. **Rosebeck, S., A. O. Rehman, P. C. Lucas, and L. M. McAllister-Lucas**. 2011. From MALT lymphoma to the CBM signalosome: three decades of discovery. Cell Cycle **10**:2485-2496. doi:16923 [pii];10.4161/cc.10.15.16923 [doi].

4. **Afonina, I. S., L. Elton, I. Carpentier, and R. Beyaert**. 2015. MALT1--a universal soldier: multiple strategies to ensure NF-kappaB activation and target gene expression. FEBS J. **282**:3286-3297. doi:10.1111/febs.13325 [doi].

5. **Hailfinger, S., H. Nogai, C. Pelzer, M. Jaworski, K. Cabalzar, J. E. Charton, M. Guzzardi, C. Decaillet, M. Grau, B. Dorken, P. Lenz, G. Lenz, and M. Thome**. 2011. Malt1-dependent RelB cleavage promotes canonical NF-kappaB activation in lymphocytes and lymphoma cell lines. Proc.Natl.Acad.Sci.U.S.A **108**:14596-14601. doi:1105020108 [pii];10.1073/pnas.1105020108 [doi].

6. **Staal, J., Y. Driege, T. Bekaert, A. Demeyer, D. Muyllaert, D. P. Van, K. Gevaert, and R. Beyaert**. 2011. T-cell receptor-induced JNK activation requires proteolytic

618 inactivation of CYLD by MALT1. EMBO J. **30**:1742-1752. doi:emboj201185
619 [pii];10.1038/emboj.2011.85 [doi].

620 7. **Coornaert, B., M. Baens, K. Heyninck, T. Bekaert, M. Haegman, J. Staal, L. Sun,**
621 **Z. J. Chen, P. Marynen, and R. Beyaert**. 2008. T cell antigen receptor stimulation
622 induces MALT1 paracaspase-mediated cleavage of the NF-kappaB inhibitor A20.
623 Nat.Immunol. **9**:263-271. doi:ni1561 [pii];10.1038/ni1561 [doi].

624 8. **Klein, T., S. Y. Fung, F. Renner, M. A. Blank, A. Dufour, S. Kang, M. Bolger-**
625 **Munro, J. M. Scurll, J. J. Priatel, P. Schweigler, S. Melkko, M. R. Gold, R. I.**
626 **Viner, C. H. Regnier, S. E. Turvey, and C. M. Overall**. 2015. The paracaspase
627 MALT1 cleaves HOIL1 reducing linear ubiquitination by LUBAC to dampen
628 lymphocyte NF-kappaB signalling. Nat.Commun. **6**:8777. doi:ncomms9777
629 [pii];10.1038/ncomms9777 [doi].

630 9. **Jeltsch, K. M., D. Hu, S. Brenner, J. Zoller, G. A. Heinz, D. Nagel, K. U. Vogel, N.**
631 **Rehage, S. C. Warth, S. L. Edelmann, R. Gloury, N. Martin, C. Lohs, M. Lech, J.**
632 **E. Stehklein, A. Geerlof, E. Kremmer, A. Weber, H. J. Anders, I. Schmitz, M.**
633 **Schmidt-Supprian, M. Fu, H. Holtmann, D. Krappmann, J. Ruland, A. Kallies, M.**
634 **Heikenwalder, and V. Heissmeyer**. 2014. Cleavage of roquin and regnase-1 by the
635 paracaspase MALT1 releases their cooperatively repressed targets to promote T(H)17
636 differentiation. Nat.Immunol. **15**:1079-1089. doi:ni.3008 [pii];10.1038/ni.3008 [doi].

637 10. **Uehata, T., H. Iwasaki, A. Vandenbon, K. Matsushita, E. Hernandez-Cuellar, K.**
638 **Kuniyoshi, T. Satoh, T. Mino, Y. Suzuki, D. M. Standley, T. Tsujimura, H.**
639 **Rakugi, Y. Isaka, O. Takeuchi, and S. Akira**. 2013. Malt1-induced cleavage of
640 regnase-1 in CD4(+) helper T cells regulates immune activation. Cell **153**:1036-1049.
641 doi:S0092-8674(13)00510-2 [pii];10.1016/j.cell.2013.04.034 [doi].

642 11. **Nagel, D., S. Spranger, M. Vincendeau, M. Grau, S. Raffegerst, B. Kloo, D. Hlahla,**
643 **M. Neuenschwander, K. J. Peter von, K. Hadian, B. Dorken, P. Lenz, G. Lenz, D.**
644 **J. Schendel, and D. Krappmann**. 2012. Pharmacologic inhibition of MALT1 protease
645 by phenothiazines as a therapeutic approach for the treatment of aggressive ABC-
646 DLBCL. Cancer Cell **22**:825-837. doi:S1535-6108(12)00482-5
647 [pii];10.1016/j.ccr.2012.11.002 [doi].

648 12. **Mc Guire, C., L. Elton, P. Wieghofer, J. Staal, S. Voet, A. Demeyer, D. Nagel, D.**
649 **Krappmann, M. Prinz, R. Beyaert, and G. van Loo**. 2014. Pharmacological
650 inhibition of MALT1 protease activity protects mice in a mouse model of multiple
651 sclerosis. J.Neuroinflammation. **11**:124. doi:1742-2094-11-124 [pii];10.1186/1742-
652 2094-11-124 [doi].

653 13. **Fontan, L., C. Yang, V. Kabaleeswaran, L. Volpon, M. J. Osborne, E. Beltran, M.**
654 **Garcia, L. Cerchietti, R. Shaknovich, S. N. Yang, F. Fang, R. D. Gascoyne, J. A.**
655 **Martinez-Climent, J. F. Glickman, K. Borden, H. Wu, and A. Melnick**. 2012.
656 MALT1 small molecule inhibitors specifically suppress ABC-DLBCL in vitro and in
657 vivo. Cancer Cell **22**:812-824. doi:S1535-6108(12)00483-7
658 [pii];10.1016/j.ccr.2012.11.003 [doi].

659 14. **Ruefli-Brasse, A. A., D. M. French, and V. M. Dixit**. 2003. Regulation of NF-
660 kappaB-dependent lymphocyte activation and development by paracaspase. Science
661 **302**:1581-1584. doi:10.1126/science.1090769 [doi];1090769 [pii].

662 15. **Ruland, J., G. S. Duncan, A. Wakeham, and T. W. Mak**. 2003. Differential
663 requirement for Malt1 in T and B cell antigen receptor signaling. Immunity. **19**:749-
664 758. doi:S1074761303002930 [pii].

16. **Brustle, A., D. Brenner, C. B. Knobbe, P. A. Lang, C. Virtanen, B. M. Hershenfield, C. Reardon, S. M. Lacher, J. Ruland, P. S. Ohashi, and T. W. Mak**. 2012. The NF-kappaB regulator MALT1 determines the encephalitogenic potential of Th17 cells. J.Clin.Invest **122**:4698-4709. doi:63528 [pii];10.1172/JCI63528 [doi].

17. **Mc Guire, C., P. Wieghofer, L. Elton, D. Muylaert, M. Prinz, R. Beyaert, and G. van Loo**. 2013. Paracaspase MALT1 deficiency protects mice from autoimmune-mediated demyelination. J.Immunol. **190**:2896-2903. doi:jimmunol.1201351 [pii];10.4049/jimmunol.1201351 [doi].

18. **Punwani, D., H. Wang, A. Y. Chan, M. J. Cowan, J. Mallott, U. Sunderam, M. Mollenauer, R. Srinivasan, S. E. Brenner, A. Mulder, F. H. Claas, A. Weiss, and J. M. Puck**. 2015. Combined immunodeficiency due to MALT1 mutations, treated by hematopoietic cell transplantation. J.Clin.Immunol. **35**:135-146. doi:10.1007/s10875-014-0125-1 [doi].

19. **McKinnon, M. L., J. Rozmus, S. Y. Fung, A. F. Hirschfeld, K. L. Del Bel, L. Thomas, N. Marr, S. D. Martin, A. K. Marwaha, J. J. Priatel, R. Tan, C. Senger, A. Tsang, J. Prendiville, A. K. Junker, M. Seear, K. R. Schultz, L. M. Sly, R. A. Holt, M. S. Patel, J. M. Friedman, and S. E. Turvey**. 2014. Combined immunodeficiency associated with homozygous MALT1 mutations. J.Allergy Clin.Immunol. **133**:1458-62, 1462. doi:S0091-6749(13)01706-5 [pii];10.1016/j.jaci.2013.10.045 [doi].

20. **Jabara, H. H., T. Ohsumi, J. Chou, M. J. Massaad, H. Benson, A. Megarbane, E. Chouery, R. Mikhael, O. Gorka, A. Gewies, P. Portales, T. Nakayama, H. Hosokawa, P. Revy, H. Herrod, D. F. Le, G. Lefranc, J. Ruland, and R. S. Geha**. 2013. A homozygous mucosa-associated lymphoid tissue 1 (MALT1) mutation in a

family with combined immunodeficiency. J.Allergy Clin.Immunol. **132**:151-158. doi:S0091-6749(13)00694-5 [pii];10.1016/j.jaci.2013.04.047 [doi].

21. **Jackson, A. C.** 2008. Rabies. Neurol.Clin. **26**:717-26, ix. doi:S0733-8619(08)00035-2 [pii];10.1016/j.ncl.2008.03.010 [doi].

22. **Roy, A. and D. C. Hooper**. 2008. Immune evasion by rabies viruses through the maintenance of blood-brain barrier integrity. J.Neurovirol. **14**:401-411. doi:905663124 [pii];10.1080/13550280802235924 [doi].

23. **Hampson, K., L. Coudeville, T. Lembo, M. Sambo, A. Kieffer, M. Attlan, J. Barrat, J. D. Blanton, D. J. Briggs, S. Cleaveland, P. Costa, C. M. Freuling, E. Hiby, L. Knopf, F. Leanes, F. X. Meslin, A. Metlin, M. E. Miranda, T. Muller, L. H. Nel, S. Recuenco, C. E. Rupprecht, C. Schumacher, L. Taylor, M. A. Vigilato, J. Zinsstag, and J. Dushoff**. 2015. Estimating the global burden of endemic canine rabies. PLoS.Negl.Trop.Dis. **9**:e0003709. doi:10.1371/journal.pntd.0003709 [doi];PNTD-D-14-00532 [pii].

24. **Hattwick, M. A., T. T. Weis, C. J. Stechschulte, G. M. Baer, and M. B. Gregg**. 1972. Recovery from rabies. A case report. Ann.Intern.Med. **76**:931-942.

25. **Willoughby, R. E., Jr., K. S. Tieves, G. M. Hoffman, N. S. Ghanayem, C. M. Amlie-Lefond, M. J. Schwabe, M. J. Chusid, and C. E. Rupprecht**. 2005. Survival after treatment of rabies with induction of coma. N.Engl.J.Med. **352**:2508-2514. doi:352/24/2508 [pii];10.1056/NEJMoa050382 [doi].

26. **Abelseth, M. K.** 1964. An Attenuated Rabies Vaccine for Domestic Animals Produced in Tissue Culture. Can.Vet.J. **5**:279-286.

27. **Abelseth, M. K.** 1964. Propagation of Rabies Virus in Pig Kidney Cell Culture. Can.Vet.J. **5**:84-87.

28. **Lawson, K. F., R. Hertler, K. M. Charlton, J. B. Campbell, and A. J. Rhodes**. 1989. Safety and immunogenicity of ERA strain of rabies virus propagated in a BHK-21 cell line. Can.J.Vet.Res. **53**:438-444.

29. **Abelseth, M. K.** 1967. Further studies on the use of ERA rabies vaccine in domestic animals. Can.Vet.J. **8**:221-227.

30. **Galelli, A., L. Baloul, and M. Lafon**. 2000. Abortive rabies virus central nervous infection is controlled by T lymphocyte local recruitment and induction of apoptosis. J.Neurovirol. **6**:359-372.

31. **Weiland, F., J. H. Cox, S. Meyer, E. Dahme, and M. J. Reddehase**. 1992. Rabies virus neuritic paralysis: immunopathogenesis of nonfatal paralytic rabies. J.Virol. **66**:5096-5099.

32. **Lafon, M., F. Megret, S. G. Meuth, O. Simon, M. L. Velandia Romero, M. Lafage, L. Chen, L. Alexopoulou, R. A. Flavell, C. Prehaud, and H. Wiendl**. 2008. Detrimental contribution of the immuno-inhibitor B7-H1 to rabies virus encephalitis. J.Immunol. **180**:7506-7515. doi:180/11/7506 [pii].

33. **Schlauderer, F., K. Lammens, D. Nagel, M. Vincendeau, A. C. Eitelhuber, S. H. Verhelst, D. Kling, A. Chrusciel, J. Ruland, D. Krappmann, and K. P. Hopfner**. 2013. Structural analysis of phenothiazine derivatives as allosteric inhibitors of the MALT1 paracaspase. Angew.Chem.Int.Ed Engl. **52**:10384-10387. doi:10.1002/anie.201304290 [doi].

34. **Wolfer, A., T. Bakker, A. Wilson, M. Nicolas, V. Ioannidis, D. R. Littman, P. P. Lee, C. B. Wilson, W. Held, H. R. MacDonald, and F. Radtke**. 2001. Inactivation of Notch 1 in immature thymocytes does not perturb CD4 or CD8T cell development. Nat.Immunol. **2**:235-241. doi:10.1038/85294 [doi].

35. **Tronche, F., C. Kellendonk, O. Kretz, P. Gass, K. Anlag, P. C. Orban, R. Bock, R. Klein, and G. Schutz**. 1999. Disruption of the glucocorticoid receptor gene in the nervous system results in reduced anxiety. Nat.Genet. **23**:99-103. doi:10.1038/12703 [doi].

36. **Clausen, B. E., C. Burkhardt, W. Reith, R. Renkawitz, and I. Forster**. 1999. Conditional gene targeting in macrophages and granulocytes using LysMcre mice. Transgenic Res. **8**:265-277.

37. **Fehlner-Gardiner, C., S. Nadin-Davis, J. Armstrong, F. Muldoon, P. Bachmann, and A. Wandeler**. 2008. Era vaccine-derived cases of rabies in wildlife and domestic animals in Ontario, Canada, 1989-2004. J.Wildl.Dis. **44**:71-85. doi:44/1/71 [pii];10.7589/0090-3558-44.1.71 [doi].

38. **Rosseels, V., F. Naze, S. De Craeye, A. Francart, M. Kalai, and S. Van Gucht.** 2011. A non-invasive intranasal inoculation technique using isoflurane anesthesia to infect the brain of mice with rabies virus. J.Virol.Methods **173**:127-136. doi:S0166-0934(11)00050-4 [pii];10.1016/j.jviromet.2011.01.019 [doi].

39. **Posel, C., K. Moller, J. Boltze, D. C. Wagner, and G. Weise**. 2016. Isolation and Flow Cytometric Analysis of Immune Cells from the Ischemic Mouse Brain. J.Vis.Exp.53658. doi:10.3791/53658 [doi].

40. **Kip, E., F. Naze, V. Suin, T. Vanden Berghe, A. Francart, S. Lamoral, P. Vandenabeele, R. Beyaert, S. Van Gucht, and M. Kalai**. 2017. Impact of caspase-1/11, -3, -7, or IL-1beta/IL-18 deficiency on rabies virus-induced macrophage cell death and onset of disease. Cell Death.Discov. **3**:17012. doi:10.1038/cddiscovery.2017.12 [doi].

41. **Brustle, A., D. Brenner, C. B. Knobbe-Thomsen, M. Cox, P. A. Lang, K. S. Lang, and T. W. Mak**. 2017. MALT1 is an intrinsic regulator of regulatory T cells. Cell Death.Differ. **24**:1214-1223. doi:cdd2015104 [pii];10.1038/cdd.2015.104 [doi].

42. **Block, M. L., L. Zecca, and J. S. Hong**. 2007. Microglia-mediated neurotoxicity: uncovering the molecular mechanisms. Nat.Rev.Neurosci. **8**:57-69. doi:nrn2038 [pii];10.1038/nrn2038 [doi].

43. **Zhang, D., X. Hu, L. Qian, J. P. O'Callaghan, and J. S. Hong**. 2010. Astrogliosis in CNS pathologies: is there a role for microglia? Mol.Neurobiol. **41**:232-241. doi:10.1007/s12035-010-8098-4 [doi].

44. **Rupprecht, C. E., L. Blass, K. Smith, L. A. Orciari, M. Niezgoda, S. G. Whitfield, R. V. Gibbons, M. Guerra, and C. A. Hanlon**. 2001. Human infection due to recombinant vaccinia-rabies glycoprotein virus. N.Engl.J.Med. **345**:582-586. doi:10.1056/NEJMoa010560 [doi].

45. **Goh, K. T.** 1999. Resurgence of mumps in Singapore caused by the Rubini mumps virus vaccine strain. Lancet **354**:1355-1356. doi:S0140673699028536 [pii].

46. **Seligman, S. J.** 2011. Yellow fever virus vaccine-associated deaths in young women. Emerg.Infect.Dis. **17**:1891-1893. doi:10.3201/eid1710.101789 [doi].

47. **Berggren, K. L., M. Tharp, and K. M. Boyer**. 2005. Vaccine-associated "wild-type" measles. Pediatr.Dermatol. **22**:130-132. doi:PDE22208 [pii];10.1111/j.1525-1470.2005.22208.x [doi].

48. **Hooper, D. C., K. Morimoto, M. Bette, E. Weihe, H. Koprowski, and B. Dietzschold**. 1998. Collaboration of antibody and inflammation in clearance of rabies virus from the central nervous system. J.Virol. **72**:3711-3719.

49. **Lebrun, A., C. Portocarrero, R. B. Kean, D. A. Barkhouse, M. Faber, and D. C. Hooper**. 2015. T-bet Is Required for the Rapid Clearance of Attenuated Rabies Virus from Central Nervous System Tissue. J.Immunol. **195**:4358-4368. doi:jimmunol.1501274 [pii];10.4049/jimmunol.1501274 [doi].

50. **Huppert, J., D. Closhen, A. Croxford, R. White, P. Kulig, E. Pietrowski, I. Bechmann, B. Becher, H. J. Luhmann, A. Waisman, and C. R. Kuhlmann**. 2010. Cellular mechanisms of IL-17-induced blood-brain barrier disruption. FASEB J. **24**:1023-1034. doi:fj.09-141978 [pii];10.1096/fj.09-141978 [doi].

51. **Chai, Q., W. Q. He, M. Zhou, H. Lu, and Z. F. Fu**. 2014. Enhancement of blood-brain barrier permeability and reduction of tight junction protein expression are modulated by chemokines/cytokines induced by rabies virus infection. J.Virol. **88**:4698-4710. doi:JVI.03149-13 [pii];10.1128/JVI.03149-13 [doi].

52. **Chai, Q., R. She, Y. Huang, and Z. F. Fu**. 2015. Expression of neuronal CXCL10 induced by rabies virus infection initiates infiltration of inflammatory cells, production of chemokines and cytokines, and enhancement of blood-brain barrier permeability. J.Virol. **89**:870-876. doi:JVI.02154-14 [pii];10.1128/JVI.02154-14 [doi].

799 53. **Hooper, D. C., T. W. Phares, M. J. Fabis, and A. Roy**. 2009. The production of
800 antibody by invading B cells is required for the clearance of rabies virus from the
801 central nervous system. PLoS.Negl.Trop.Dis. **3**:e535. doi:10.1371/journal.pntd.0000535
802 [doi].

803 54. **Huang, C. T., Z. Li, Y. Huang, G. Zhang, M. Zhou, Q. Chai, H. Wu, and Z. F. Fu**.
804 2014. Enhancement of blood-brain barrier permeability is required for intravenously
805 administered virus neutralizing antibodies to clear an established rabies virus infection
806 from the brain and prevent the development of rabies in mice. Antiviral Res. **110**:132-
807 141. doi:S0166-3542(14)00212-5 [pii];10.1016/j.antiviral.2014.07.013 [doi].

808 55. **Unger, J. W.** 1998. Glial reaction in aging and Alzheimer's disease. Microsc.Res.Tech.
809 **43**:24-28. doi:10.1002/(SICI)1097-0029(19981001)43:1<24::AID-JEMT4>3.0.CO;2-P
810 [pii];10.1002/(SICI)1097-0029(19981001)43:1<24::AID-JEMT4>3.0.CO;2-P [doi].

811 56. **Sawada, M., K. Imamura, and T. Nagatsu**. 2006. Role of cytokines in inflammatory
812 process in Parkinson's disease. J.Neural Transm.Suppl373-381.

813 57. **Noseworthy, J. H., C. Lucchinetti, M. Rodriguez, and B. G. Weinshenker**. 2000.
814 Multiple sclerosis. N.Engl.J.Med. **343**:938-952. doi:10.1056/NEJM200009283431307
815 [doi].

816 58. **Tarkowski, E., L. Rosengren, C. Blomstrand, C. Wikkelso, C. Jensen, S. Ekholm,**
817 **and A. Tarkowski**. 1997. Intrathecal release of pro- and anti-inflammatory cytokines
818 during stroke. Clin.Exp.Immunol. **110**:492-499.

819 59. **Najjar, S., D. M. Pearlman, K. Alper, A. Najjar, and O. Devinsky**. 2013.
820 Neuroinflammation and psychiatric illness. J.Neuroinflammation. **10**:43. doi:1742-
821 2094-10-43 [pii];10.1186/1742-2094-10-43 [doi].

822 60. **Depino, A. M.** 2013. Peripheral and central inflammation in autism spectrum disorders.
823 Mol.Cell Neurosci. **53**:69-76. doi:S1044-7431(12)00185-6
824 [pii];10.1016/j.mcn.2012.10.003 [doi].
825
826

827 **FIGURE LEGENDS**

828

829 **Figure 1. MALT1 is critical to control the pathogenicity of ERA virus.** MALT1$^{-/-}$ (n = 10)
830 and MALT1$^{+/+}$ littermates (n =10) were infected intranasally with ERA virus. **(A)** Clinical
831 symptoms and **(B)** survival rates were assessed. All MALT1$^{-/-}$ mice developed severe disease
832 and had to be euthanized. MALT1$^{+/+}$ mice developed only mild symptoms. Results are
833 representative of 2 independent experiments.

834

835 **Figure 2. Virus spread in the brain of MALT1$^{-/-}$ and MALT1$^{+/+}$ mice following**
836 **intranasal inoculation. (A)** Schematic overview of the experiment. Mice were inoculated
837 intranasally with the ERA virus and sacrificed at 10, 17 and 35 DPI. **(B)** Profile of viral RNA
838 load in total brain determined by RT-qPCR. **(C, D)** Profile of viral RNA load in different
839 parts of the brain (**= P-value $\leq$ 0.01). **(E)** Immunofluorescence staining for viral
840 nucleocapsid in the brain tissue. At 10 DPI, green fluorescent spots indicate the abundant
841 spread of virus in the brain of MALT1$^{-/-}$ and MALT1$^{+/+}$ mice. At 17 DPI, only a small
842 amount of viral antigens were still visible in MALT1$^{+/+}$ mice, whereas viral antigens were
843 still abundant in the brains of MALT1$^{-/-}$ mice. These results are representative of 3 mice per
844 time point and per genotype. Scale bars represent 20µm, magnification 40×.

845

846 **Figure 3. Defective expression of anti-viral and inflammatory genes in the brain of ERA**
847 **virus-infected MALT1$^{-/-}$ mice.** Quantitative RT-qPCR measurements of the indicated
848 mRNA expression levels in brains of MALT1$^{+/+}$ (n=7) and MALT1$^{-/-}$ littermate mice (n=7) at
849 10 DPI and 17 DPI are shown. Results are represented as fold increase compared to
850 respectively non-infected MALT1$^{+/+}$ and MALT1$^{-/-}$ littermate mice. Differences in the fold
851 increase at the same time point were determined by two-way ANOVA and Sidak's multiple-

852 comparison test and statistical differences between MALT1$^{+/+}$ and MALT1$^{-/-}$ mice are
853 denoted as ****, ***, **, and *, representing P-values of less than 0.0001, 0.001, 0.01 and
854 0.05, respectively.
855
856 **Figure 4. Reduced infiltration and activation of inflammatory cells in the brain of**
857 **MALT1$^{-/-}$ mice at 10 DPI with ERA virus.** Immunohistochemical analysis of CNS sections
858 from ERA-infected MALT1$^{+/+}$ and MALT1$^{-/-}$ mice at 10 and 17 DPI. PBS-inoculated
859 MALT1$^{+/+}$ mice were used as controls. Sections of cerebellum and hippocampus are shown.
860 Brain sections were immunostained for Iba-1 (microglial cells), CD3 (T cells), Mac-3
861 (macrophages), B220 (B cells) and GFAP (astrocytes). PBS-injected mice showed abundant
862 inactive ramified microglial cells and astrocytes, but no B cell, macrophage or T cell
863 infiltration. At 10 DPI, ERA virus-infected MALT1$^{+/+}$ mice showed activation of microglia
864 and astroglia cells, infiltration of T lymphocytes and macrophages in the parenchyma, and
865 infiltration of B cells around the blood vessels and choroid plexus. In MALT1$^{-/-}$ mice, T
866 lymphocyte and macrophage infiltration, as well as microglial activation, were reduced at 10
867 DPI. Moreover, B cells could not be observed around the blood vessels or choroid plexus in
868 MALT1$^{-/-}$ mice. At 17 DPI, pronounced microglial activation and T lymphocyte infiltration
869 were observed in both MALT1$^{+/+}$ and MALT1$^{-/-}$ mice. Macrophages were no longer visible.
870 Astrogliosis increased further, but was more pronounced in MALT1$^{+/+}$ than in MALT1$^{-/-}$
871 mice. Scale bars represent 20µm (magnification 20×), 50µm (magnification 10x) or 100µm
872 (magnification 4×). Data are representative of two mice per condition.
873
874 **Figure 5. Flow cytometric analysis of immune cell activation and infiltration in the**
875 **brain of ERA-infected mice.** Immune cells were isolated from the brains of naïve mice and
876 infected mice (MALT1$^{+/+}$ and MALT1$^{-/-}$) at 10 DPI. **(A)** Absolute numbers of leukocytes

present in the brain were first determined and total numbers of each cell type were determined by the percentage of marker expression on total number of leukocytes. A significant decrease of total leukocytes was observed in ERA-infected MALT1$^{-/-}$ mice compared to infected MALT1$^{+/+}$ mice. **(B)** CD49b and CD3 markers were used to distinguish NK cells (CD49b$^{+}$CD3$^{-}$), NKT cells (CD49b$^{+}$CD3$^{+}$) and T cells (CD49b$^{-}$CD3$^{+}$). CD8 and CD4 markers were also used. A significant decrease of NK cells, NKT cells and CD8$^{+}$T cells was observed in ERA infected MALT1$^{-/-}$ mice compared to infected MALT1$^{+/+}$ mice. **(C)** CD45 and CD11b markers were used to distinguish T cells (CD3$^{+}$CD11b$^{-}$CD45$^{high}$), microglial cells (CD11b$^{+}$CD45$^{int}$) and monocytes/macrophages/DCs (CD11b$^{+}$CD45$^{high}$). CD45$^{int}$ cells were selected to analyze microglial activation by using CD11b and CD86, a co-stimulatory molecule expressed on activated antigen presenting cells. CD45$^{high}$ cells were selected to analyze monocyte, macrophage and DC activation. Activation of microglial cells and monocytes/macrophages/DCs was determined by CD86 expression represented as mean fluorescence intensity (MFI). A significant decrease of CD86 MFI was observed in ERA infected MALT1$^{-/-}$ mice compared to MALT1$^{+/+}$ mice, which corresponds to the dot plots. Dot plots are representative of 5 mice per condition. Statistical differences between MALT1$^{+/+}$ and MALT1$^{-/-}$ mice were determined using student t-test and are denoted as follows: ***, **, and *, representing P-values of less than 0.001, 0.01 and 0.05, respectively.

**Figure 6. Reduced granzyme B, IL-17 and IFN-γ production in T cells from ERA-infected MALT1$^{-/-}$ mice.** Immune cells were isolated from the brains of naïve mice and infected mice (MALT1$^{+/+}$ and MALT1$^{-/-}$) at 10 DPI and stained for the intracellular markers IFN-γ, IL-17 and granzyme B. T cells were gated for their phenotypic marker CD3. **(A-B)** FACS analysis revealed less production of IL-17, granzyme B and IFN-γ in T cells of ERA-infected MALT1$^{-/-}$ mice compared to ERA-infected MALT1$^{+/+}$ mice. Dot plots are

representative of 5 mice per condition. **(C)** A significant decrease of T cells expressing IFN-γ, granzyme B and IL-17 was observed in infected MALT1$^{-/-}$ mice compared to infected MALT1$^{+/+}$ mice. Statistical differences between MALT1$^{+/+}$ and MALT1$^{-/-}$ mice were determined using student t-test and are denoted as follows: ***, **, and *, representing P-values of less than 0.001, 0.01 and 0.05, respectively.

**Figure 7. Defective humoral immune response in MALT1$^{-/-}$ mice.** In MALT1$^{+/+}$ mice, antibody production was first detected in 1 out 7 mice at 10 DPI. At 17 DPI, neutralizing antibodies were detected in all MALT1$^{+/+}$ mice (n=7) and antibody levels increased further at 35 DPI (n=7). Neutralizing antibodies were not detected in MALT1$^{-/-}$ mice (n=7) at 10 DPI and in 5 out 7 mice at 17 DPI. The two remaining MALT1$^{-/-}$ mice had low levels of antibodies just above the cut off at 17 DPI.

**Figure 8. Transfer of neutralizing antibodies does not rescue MALT1$^{-/-}$ mice. (A)** Schematic overview of the experimental set-up. MALT1$^{+/+}$ mice were inoculated intranasally with the ERA virus and sacrificed at 35 DPI. Immune sera were collected, pooled, heat-inactivated and titrated prior to i.p. transfer in MALT1$^{-/-}$ mice at 10 DPI (500µl, 4.8 IU/ml). **(B)** Survival of infected mice. All MALT1$^{-/-}$ mice developed severe disease and had to be euthanized, despite transfer of immune serum.

**Figure 9. Impact of specific MALT1 deficiency in T cells, myeloid cells or cells from neuroectodermal origin on ERA virus infection. (A)** Schematic overview of conditional MALT1$^{-/-}$ mice generation. Mice expressing the CRE recombinase gene under the influence of the CD4, LysM, or Nestin promotor, were crossed with MALT1$^{FL/FL}$ mice to generate conditional mice lacking MALT1 in T cells, myeloid cells, or cells from neuroectodermal origin, respectively. Conditional mice and their wild-type littermates were genotyped and

selected for each experiment. **(B)** Survival of infected mice. Mice were infected intranasally with ERA virus and followed for disease development and survival. Mice lacking MALT1 in cells from neuro-ectodermal origin (Nestin-Cre$^{tg/+}$ MALT1$^{FL/FL}$) and myeloid cells (LysM-Cre$^{tg/+}$ MALT1$^{FL/FL}$) developed only mild disease, comparable to their wild-type littermates. Mice lacking MALT1 in T-cells (CD4-Cre$^{tg/+}$ MALT1$^{FL/FL}$) presented the same phenotype as the full MALT1$^{-/-}$ and developed severe disease requiring euthanasia at 15 DPI. **(C)** Virus neutralizing antibodies in serum. Except for one, all CD4-Cre$^{tg/+}$ MALT1$^{FL/FL}$ mice failed to mount protective levels of neutralizing antibodies. **(D)** Viral RNA in total brain. All T cell specific MALT1$^{-/-}$ mice (CD4-Cre$^{tg/+}$ MALT1$^{FL/FL}$) presented a high viral load at 15 DPI, comparable to full MALT1$^{-/-}$ mice.

**Figure 10. Treatment with mepazine in ERA-infected MALT1$^{+/+}$ mice: impact on survival, viral load and neutralizing antibody production. (A)** Schematic overview of the experimental set-up. MALT1$^{+/+}$ mice were treated daily with mepazine (n=7) or a control solution (0.9% NaCl) (n=7) starting at day -2 before virus inoculation until the end of the experiment. Two days after the first treatment, mice were inoculated intranasally with ERA virus and followed daily for signs of disease. **(B)** Survival curves. Four out of seven mepazine-treated mice developed severe disease and had to be euthanized. Control mice and the remaining 3 mepazine-treated mice survived the infection. **(C)** Profile of viral RNA in total brain of mepazine-treated MALT1$^{+/+}$ mice (n=7) and control mice (n=7) at sacrifice determined by RT-qPCR. Mepazine-treated mice with severe disease had higher viral loads. **(D)** Humoral immune response in mepazine-treated mice and control mice. Mepazine-treated mice with severe disease had no neutralizing antibodies. Control mice and the 3 surviving mepazine-treated mice had developed protective levels of neutralizing antibodies. Results are obtained from one experiment.

**Figure 11. Hypothetical model for the impact of MALT1 inactivation on ERA virus-induced immune responses in the brain.** In MALT1$^{+/+}$ mice, virus-infected neuronal cells produce CXCL10 (as shown in other studies), leading to the activation of microglia and recruitment of CXCR3-expressing T cells and NK cells to the brain parenchyma. Activated microglia and astrocytes start to produce pro-inflammatory cytokines, iNOS and CXCL10, which amplifies the recruitment and activation of several immune cell types. Activated macrophages migrate to the cervical lymph nodes, where they serve as antigen-presenting cells for naïve T cells and trigger the differentiation to effector T cells, mainly CD4$^+$ Th1 and Th17 subsets and cytotoxic CD8$^+$ T cells. Only activated T cells can infiltrate the brain. IFN-γ producing CD8$^+$T cells are the main T-cells recruited to the site of infection. Th1 cells and CD8$^+$T cells can further activate macrophages by IFN-γ production and antigen-presenting cells can reactivate the T cells that have entered the brain. CD8$^+$T cells also produce granzyme B, mediating their cytotoxic activity and virus clearance. Th1 cells provide help for B cell activation and Ig production outside the brain, whereas Th17 cells produce IL-17, contributing to the activation of microglia and astrocytes, as well as enhancing blood brain barrier permeability. The impact of MALT1 deficiency is represented by orange arrows. MALT1 deficiency in T cells reduces their activation and differentiation by antigen-presenting cells in the periphery, resulting in less effector T cells entering the brain. This does not only cause less IFN-γ and IL-17 production, but also lower T cell help to activate B cells and CD8$^+$ cytotoxic T cells, leading to defective production of virus neutralizing antibodies and reduced killing of virus-infected cells. As a consequence, viral load in the brain increases, exacerbating disease development.

A

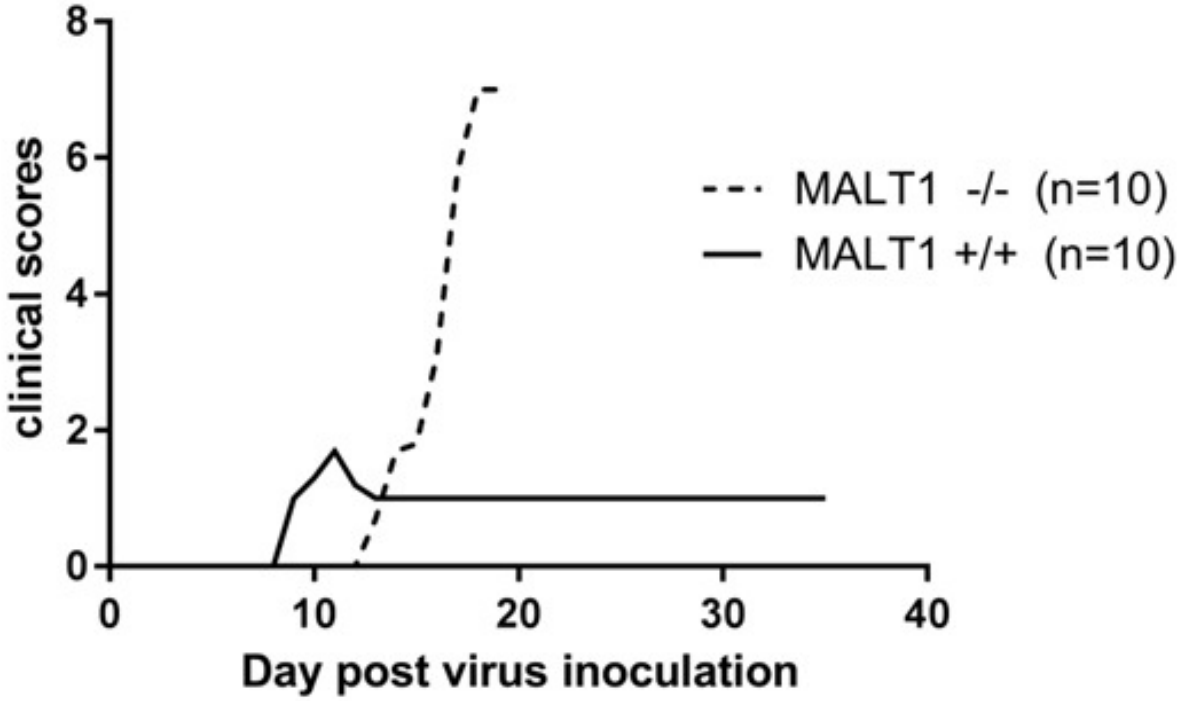


B

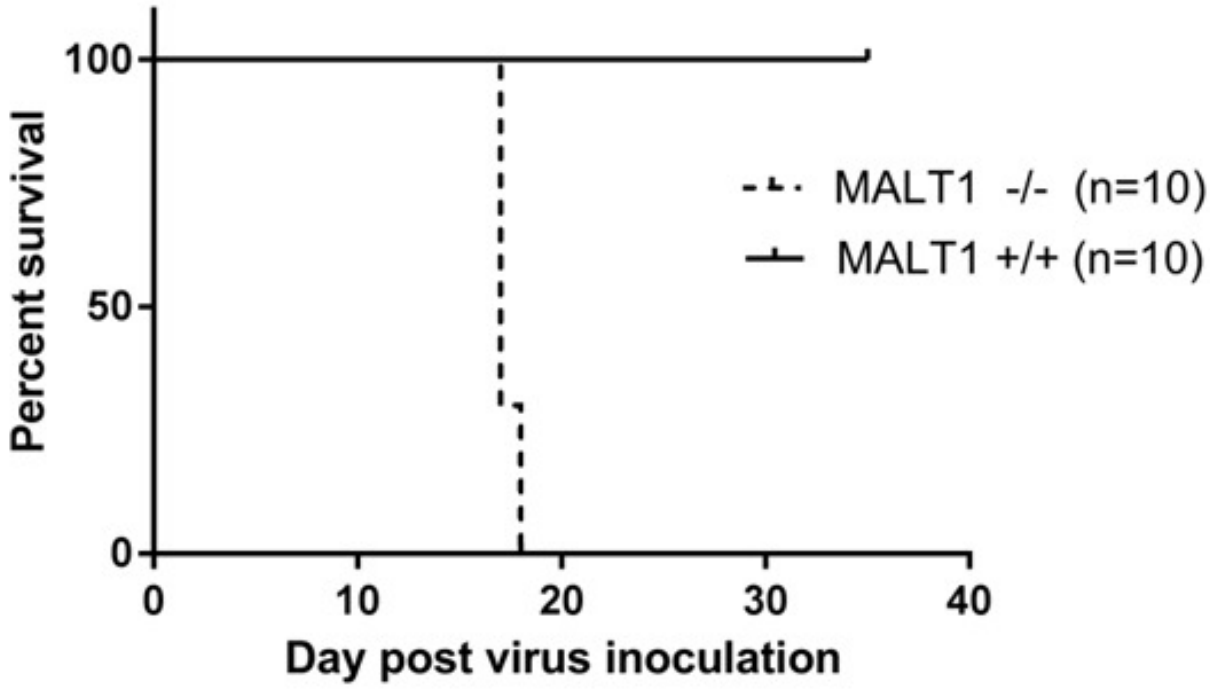

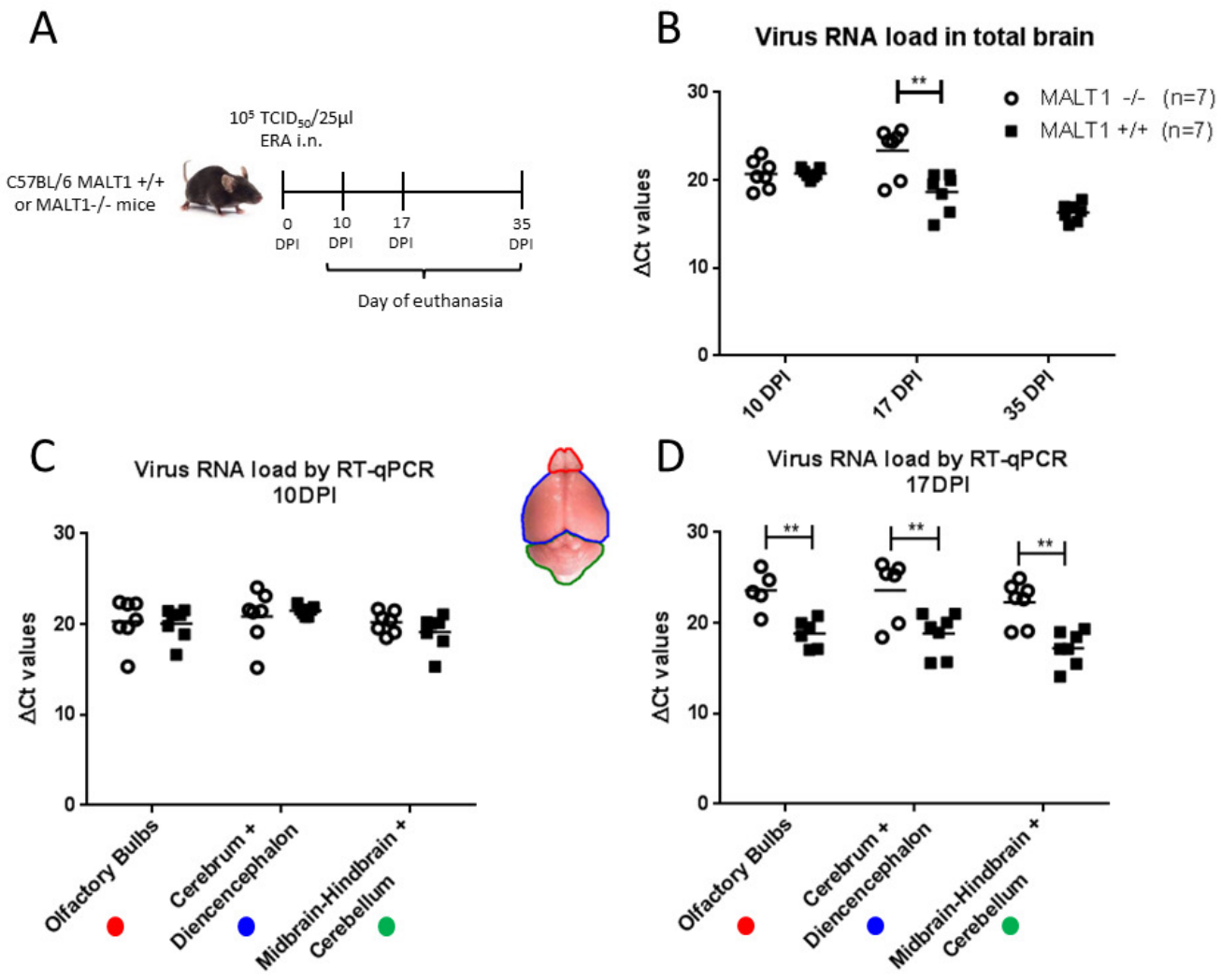

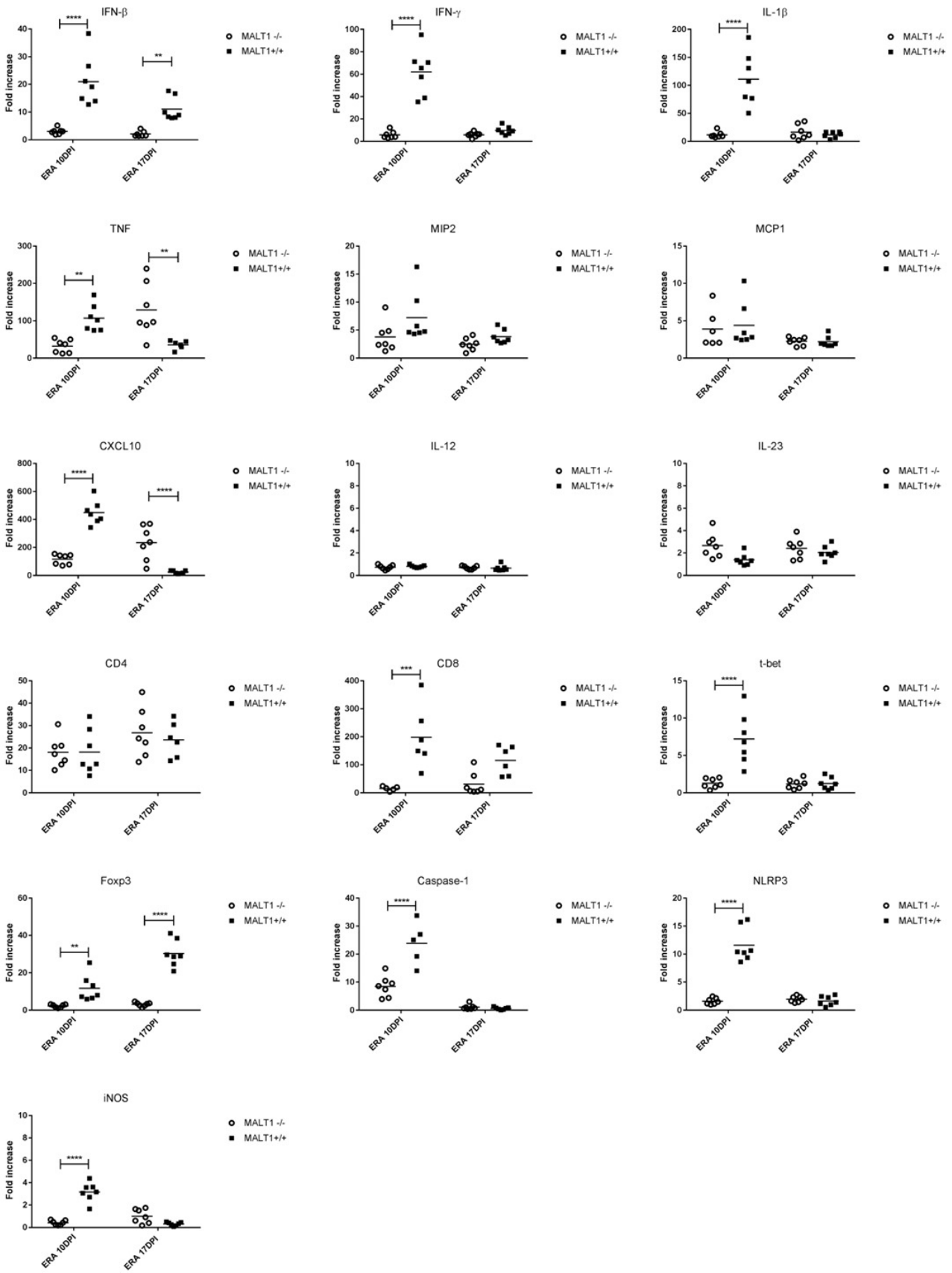

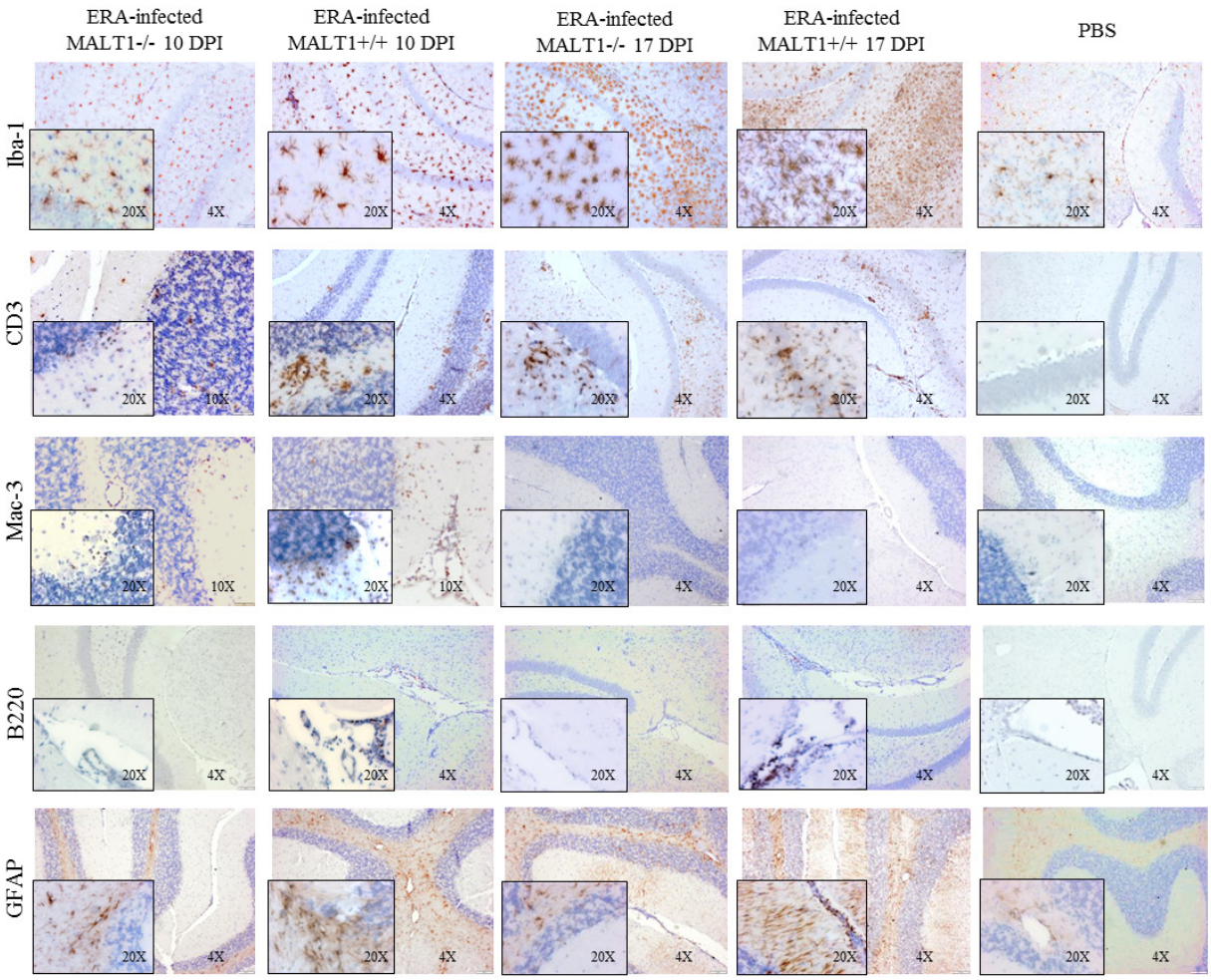






Journal of Virology

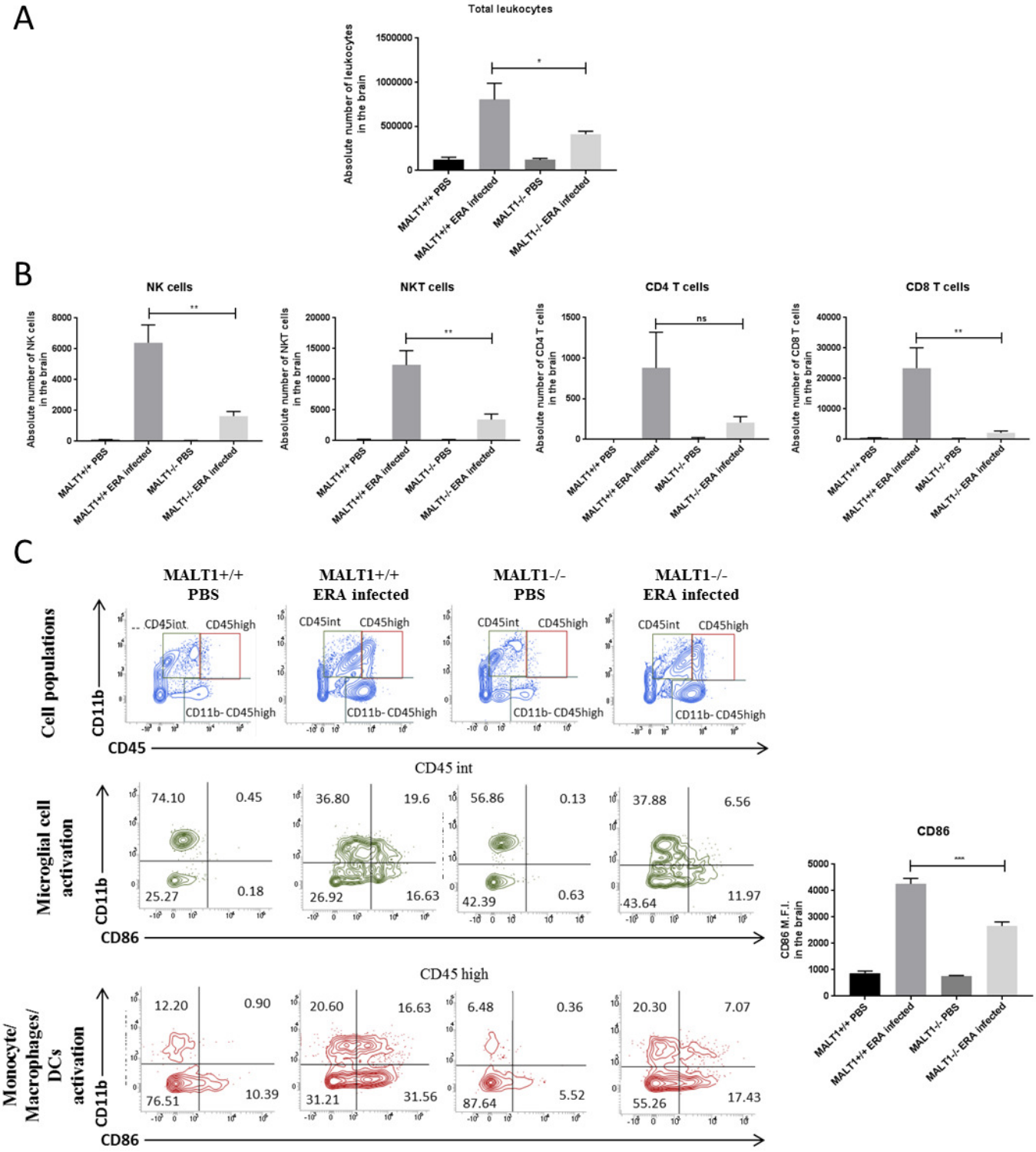

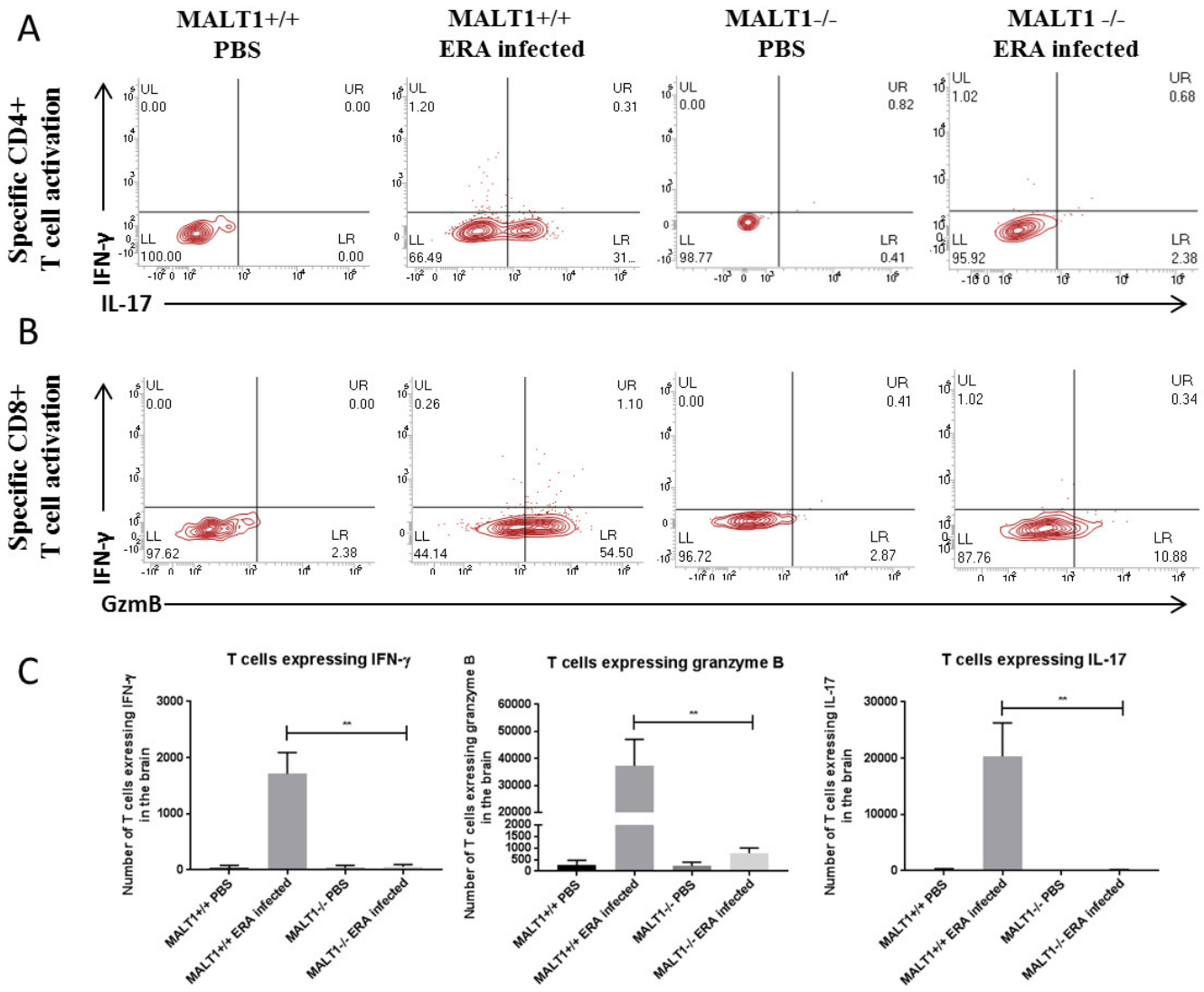

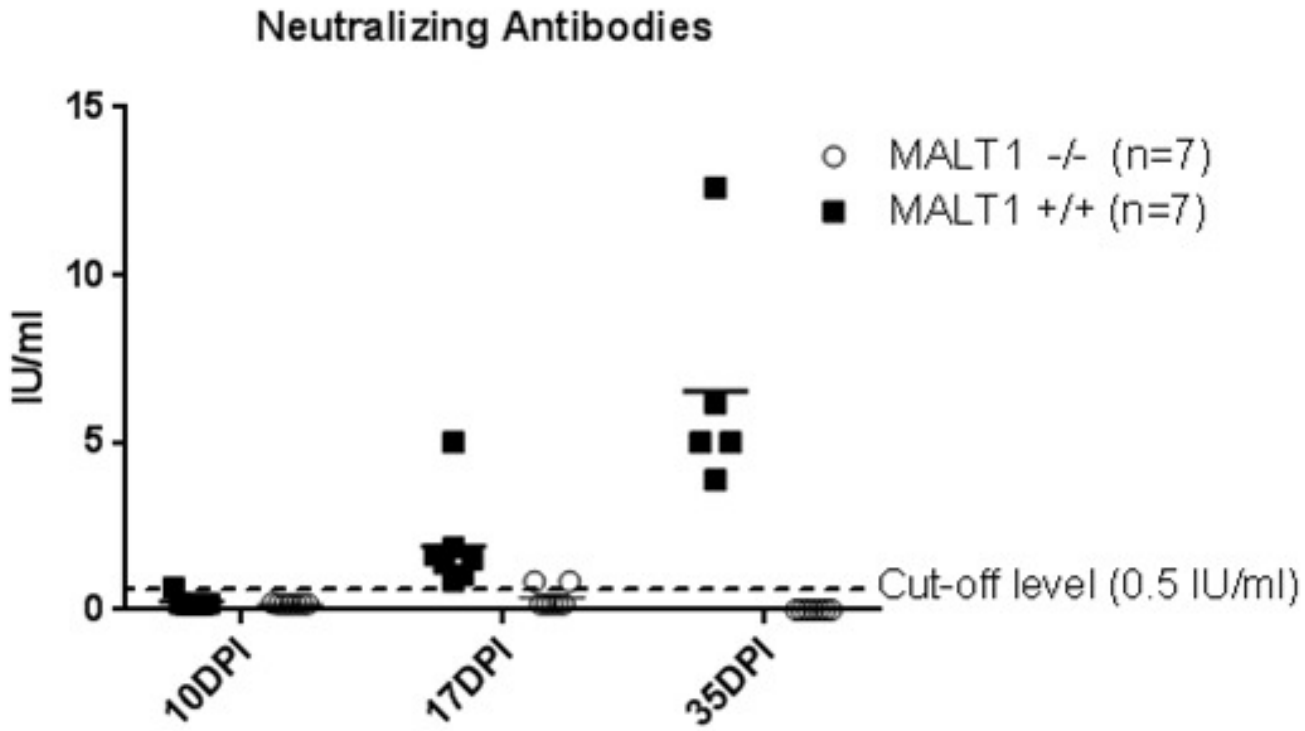




Journal of Virology
JVI
Journal of Virology

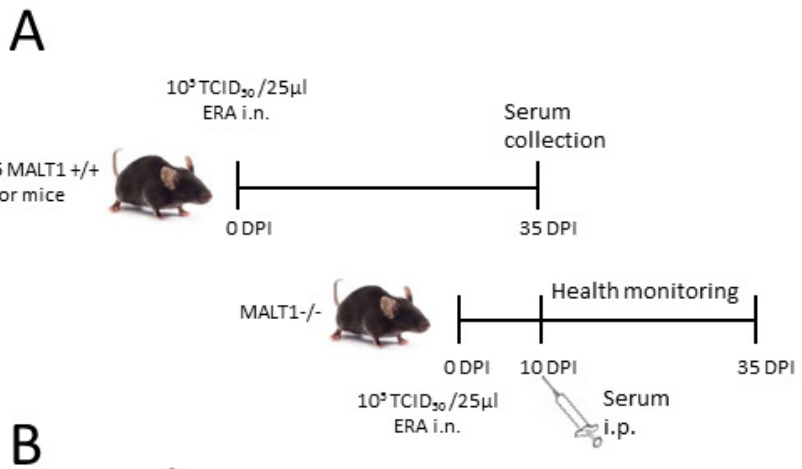


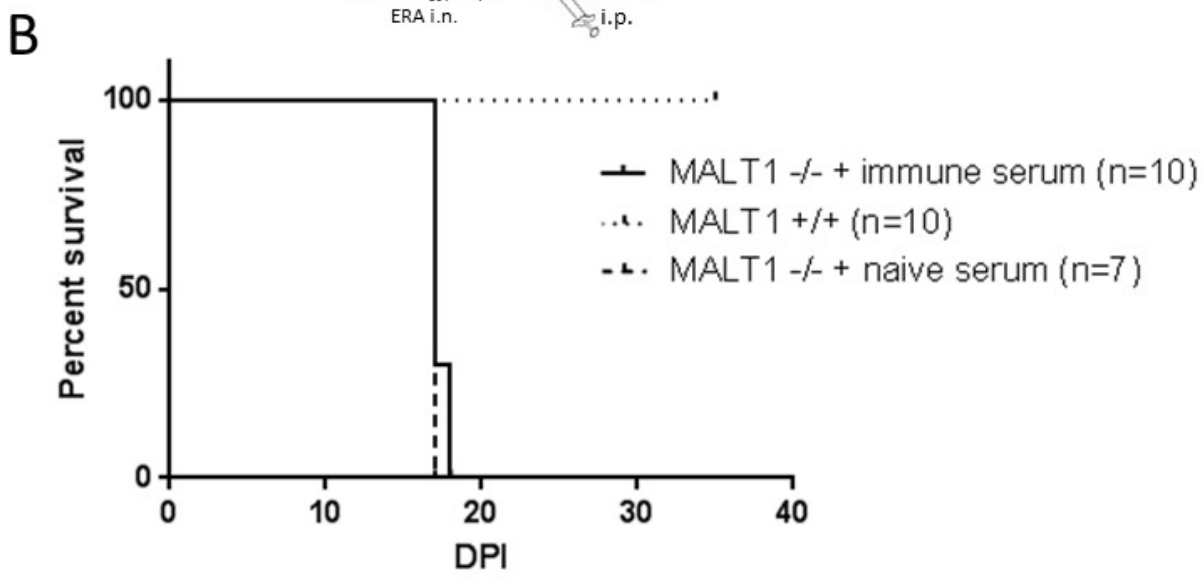

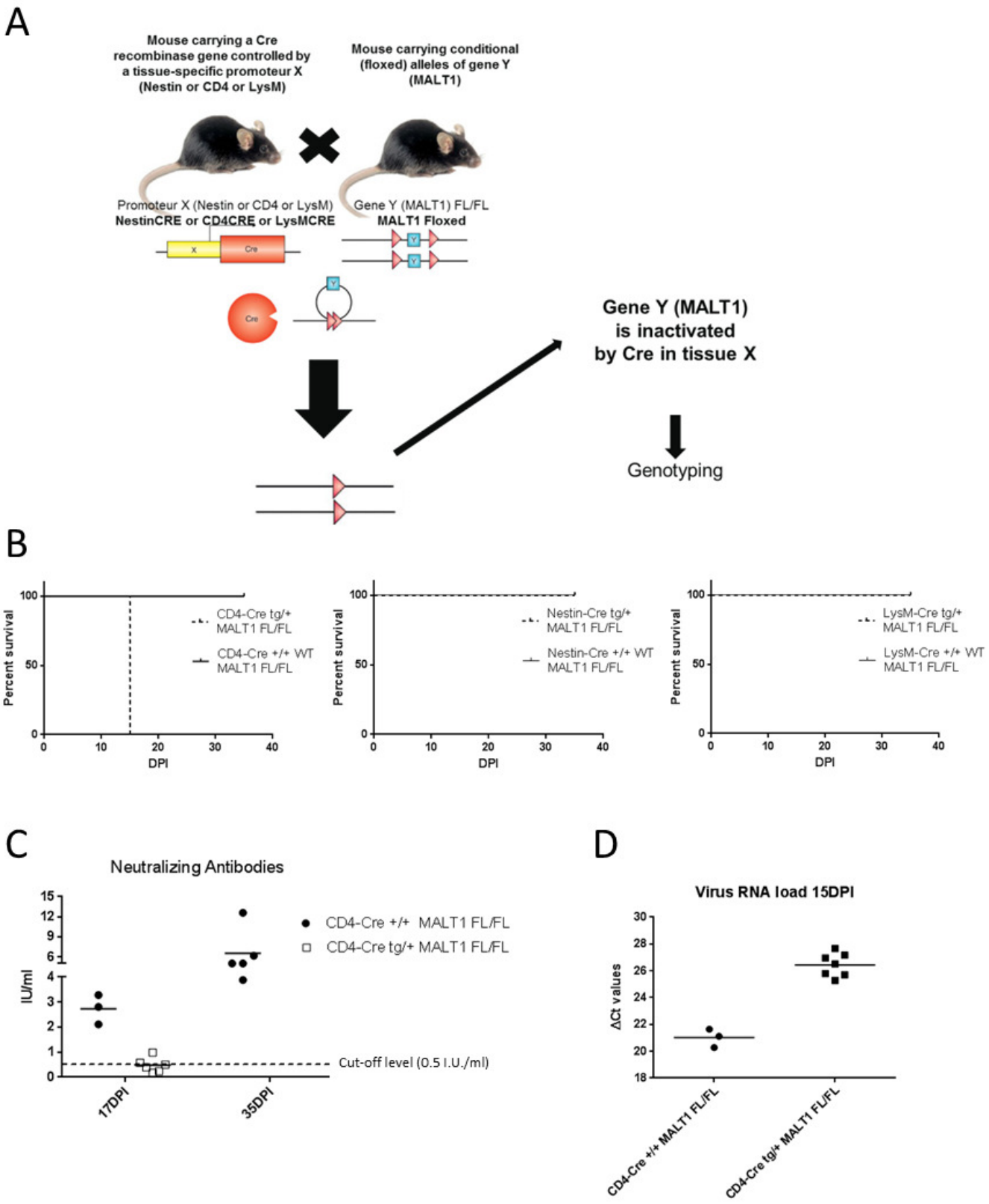

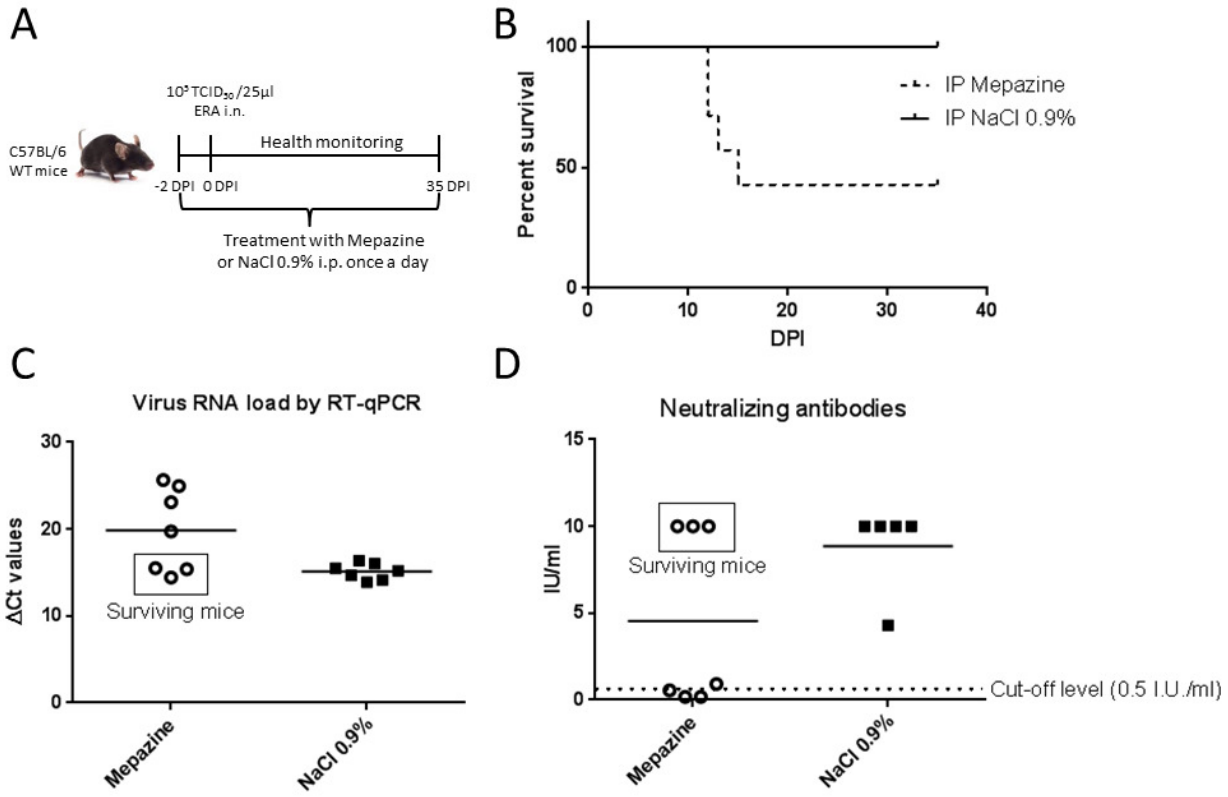

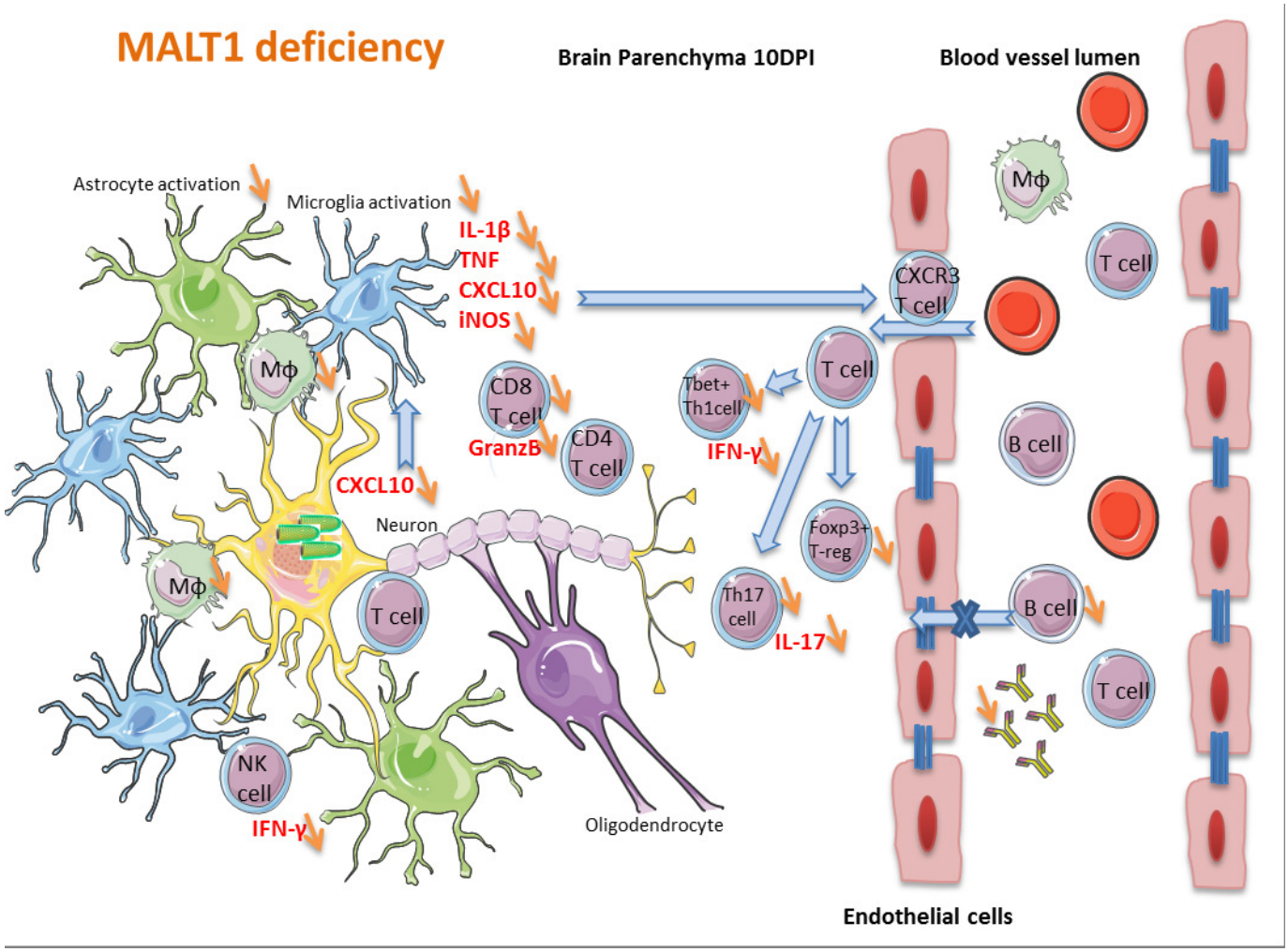






Journal of Virology

**Table 1. List of primers used in real-time PCR**

| Gene | Definition | Primer sequences |
|---|---|---|
| **RABV N** | Rabies virus nucleoprotein | F : 5'-TGGGCATAGTTGTCACTGCTTA-3'<br>R : 5'-CTCCTGCCCTGGCTCAA-3' |
| **IFN-β** | Interferon beta | F : 5'-GTTACACTGCCTTTGCCATCC-3'<br>R : 5'-CAACAATAGTCTCATTCCACCCAG-3' |
| **IFN-γ** | Interferon gamma | F : 5'-GGCTGTCCCTGAAAGAAAGC-3'<br>R : 5'-AGCGAGTTATTTGTCATTCGG-3' |
| **IL-1β** | Interleukin 1 beta | F : 5'-GCAACTGTTCCTGAACTCAAC-3'<br>R : 5'-ATCTTTTGGGGTCCGTCAACT-3' |
| **TNF** | Tumor necrosis factor | F : 5'-ACCCTCACACTCAGATCATC-3'<br>R : 5'-GAGTAGACAAGGTACAACCC-3' |
| **IL-12p35** | Interleukin 12A (p35 gene) | F : 5'-CCAAGGTCAGCGTTCCAACA-3'<br>R : 5'-AGAGGAGGTAGCGTGATTGACA-3' |
| **IL-23p19** | Interleukin 23 p19 subunit | F : 5'-CCGGGAGACCCAACAGATG-3'<br>R : 5'-CGAAGGATCTTGGAACGGAGAAG-3' |
| **MIP-2** | Macrophage inflammatory protein 2 or chemokine (C-X-C motif) ligand 2 (CXCL2) | F : 5'-CCGTCATGGATGTCTACGTG-3'<br>R : 5'-CAGCAGCAGGATACCACTGA-3' |
| **MCP-1** | Monocyte chemoattractant protein 1or chemokine (C-C motif) ligand 2 (CCL2) | F : 5'-AGTGTGAGGCAGAGAGCCAGCAT-3'<br>R : 5'-TGGATGGAAGTCTCCTGCGTGGA-3' |
| **iNOS** | Nitric oxide synthase 2, inducible | F : 5'-TGCATGGACCAGTATAAGGCAAGC-3'<br>R : 5'-GCTTCTGGTCGATGTCATGAGCAA-3' |
| **Foxp3** | Forkhead box P3 | F : 5'-TTCCTTCCCAGAGTTCTTCC-3'<br>R : 5'-CTCAAATTCATCTACGGTCCAC-3' |
| **NLRP3** | NLR family pyrin domain containing 3 | F : 5'-GCTCCAACCATTCTCTGACC-3'<br>R : 5'-AAGTAAGGCCGGAATTCACC-3' |
| **Caspase-1** | Caspase-1/Interleukin-1 converting enzyme (ICE) | F : 5'-TATGGACAAGGCACGGGACCTATG-3'<br>R : 5'-CCAGCAGCAACTTCATTTCTCTG-3' |
| **CXCL10** | Chemokine (C-X-C motif) 10 or Interferon gamma-induced protein 10 (IP-10) | F : 5'-TTCTGCCTCATCCTGCTG-3'<br>R : 5'-AGACATCTCTGCTCATCATTC-3' |
| **t-bet** | T-box transcription factor TBX21 | F : 5'-AGAACGCAGAGATCACTCAG-3'<br>R : 5'-GGATACTGGTTGGATAGAAGAGG-3' |
| **CD4** | Cluster of differentiation 4 | F : 5'-TTAATTAGAGGAGGTTCGCC-3'<br>R : 5'-ACACTCGACCTCTTGTCC-3' |
| **CD8** | Cluster of differentiation 8 | F : 5'-GTATCATGAATGTGAAGCCA-3'<br>R : 5'-CTGACACCAACTACAGGAAG-3' |